COMPUTER VISION ASSISTED GRADING OF WHEAT

by

Michael Neuman

A thesis
presented to the University of Manitoba
in partial fulfillment of the
requirements for the degree of
Master of Science
in
Electrical Engineering

Winnipeg, Manitoba

ISBN 0-315-33904-7

COMPUTER VISION ASSISTED GRADING OF WHEAT

BY

MICHAEL NEUMAN

A thesis submitted to the Faculty of Graduate Studies of the University of Manitoba in partial fulfillment of the requirements of the degree of

MASTER OF SCIENCE

I hereby declare that I am the sole author of this thesis.

I authorize the University of Manitoba to lend this thesis to other institutions or individuals for the purpose of scholarly research.

Michael Neuman

I further authorize the University of Manitoba to reproduce this thesis by photocopying or by other means, in total or in part, at the request of other institutions or individuals for the purpose of scholarly research.

Michael Neuman

The University of Manitoba requires the signatures of all persons using or photocopying this thesis. Please sign below, and give address and date.

ABSTRACT

This thesis describes the application of shape analysis methodologies for the purpose of grading wheat. Shape descriptors and metric properties of objects of interest to the wheat grading process were computed and compared. The Fourier descriptor, moment method and moment invariant techniques of shape representation were applied to the problem.

The properties so determined were evaluated for their capacity to discriminate between classes, varieties and grades of wheat and admixture elements affecting wheat grades. Various specific pattern recognition problems were posed. Stepwise discriminant analysis was applied to select the most discriminatory features. Linear discriminant functions were generated to evaluate the results of optimal decision-theoretic classification.

Discrimination of Hard Red Spring wheats from cereal grains which most frequently contaminate wheat samples was achieved. It was also possible to distinguish certain classes and cultivars of wheat from others. Visibly unsound kernels were separable from mature vitreous kernels. The usefulness of the methods and results are discussed.

ACKNOWLEDGEMENTS

I am deeply indebted to my parents, Muriel and Norman Neuman, for their support throughout this project. The contributions of the other members of the Computer-Vision Assisted Wheat Grading Group, Ed Wright, Harry Sapirstein and Dr. W. Bushuk, are greatly appreciated. Finally, I would like to thank Dr. Ed Schwedyk for his able supervision of the research conducted for this thesis.

LIST OF TABLES

LIST OF FIGURES

CONTENTS

Chapter I

APPLICATION OF MACHINE VISION TO WHEAT GRADING

1.1 INTRODUCTION

The wheat inspection process may be significantly assisted by computer vision. A human inspector might be relieved of the burden of counting objects in samples of wheat which in part determine its grade. Greater accuracy and better statistical estimates of such objects might be achieved. Objective measurements of certain attributes such as kernel vitreousness may be possible which have not previously been so.

Primary grading determinants for Red Spring Wheat are shown in Table 1.1 reproduced from the Official Grain Grading Guide (hereafter referred to as OGGG, 1985 Ed.). Identification and enumeration of objects of the categories shown is necessary and almost sufficient to achieve grading. The identification of a kernel as, say, belonging to a non-prescribed variety of wheat is a classic problem of pattern recognition. The solution of a set of such subproblems could eventually enable automatic grading of a majority of samples.

Table 1.1
RED SPRING WHEAT - PRIMARY GRADE DETERMINANTS

Grade Name	Min. Kg/hl	Variety	Degree of Soundness	Minimum Hard Vitreous Kernels	Foreign Material		W.O.O.C. or Non-prescribed Varieties		Sprouted	Bin-burnt Severe Mildew Rotted Mouldy	Heated Incl. Bin-burnt	Fire-burnt	Stones	Ergot	Sclerotinia	Smudge	Total Smudge and Black-point
					F.M. Excluding Other Cereal Grains	Total Including Other Cereal Grains	Contrasting Classes	Total Incl. Cont. Classes									
No. 1 C.W. Red Spring	75.0	Any prescribed variety of red spring wheat equal to Marquis	Reasonably well matured, reasonably free from damaged kernels	65.0%	About 0.2% includes max. 20K inseparable seeds	About 0.75%	About 1.0%	3.0% incl. not more than 1.0% non-prescribed varieties	0.5%	2K	0.1%	Nil	3K	3K	3K	30K	10.0%
No. 2 C.W. Red Spring	73.0	Any prescribed variety of red spring wheat equal to Marquis	Fairly well matured may be moderately bleached, or frost damaged, but reasonably free from severely weather damaged kernels	35.0%	About 0.5% includes max. 50K inseparable seeds	About 1.5%	About 3.0%	6.0% incl. not more than 2.0% non-prescribed varieties	1.5%	5K	0.75%	Nil	3K	8K	8K	1.0%	20.0%
No. 3 C.W. Red Spring	69.0	Any prescribed variety of red spring wheat	Excluded from higher grades on account of frosted, immature or otherwise damaged kernels	No Minimum	About 0.5% includes max. 100K inseparable seeds	About 3.5%	About 5.0%	10.0% incl not more than 5.0% non-prescribed varieties	5.0%	10K	2.0%	Nil	5K	24K	24K	5.0%	35.0%
Canada Feed Wheat	No Minimum	Any prescribed or non-prescribed variety of wheat	Excluded from all other grades on account of light weight or damage. May contain 10% heat damage but shall be reasonably sweet	No Minimum	1.0% includes max. 1.0% inseparable seeds	10.0%	No Limit	No Limit	No Limit	10.0%	10.0%	2.0%	10K	0.25%	0.25%	No Limit	No Limit
Final Grade Name	Can. Feed Wheat			No. 3 C.W. Red Spring	Over 1.0% grade Wheat, Sample C. W. Account Admixture (Inseparable Seeds) (class)	Over 10.0% grade Mixed Grain, No. 1 C.W.	Canada Feed Wheat	Canada Feed Wheat	Canada Feed Wheat	Over 10.0% grade Wheat, Sample C. W. Account Heated (class)		Over 2.0% grade Wheat, Sample C.W. Account Fire-burnt (class)	Over grade tolerance up to 2.5% grade Rejected "grade" Account Stones. Over 2.5% grade Wheat Sample Salvage	Over 0.25% grade Wheat, Sample C.W. Account Ergot (class)	Over 0.25% grade Wheat, Sample C.W. Account Admixture (Sclerotinia) (class)	Canada Feed Wheat	Canada Feed Wheat

NOTE: THE LETTER "K" IN THESE TABLES REFERS TO KERNELS OR KERNEL SIZE PIECES IN 500 GRAMS

Table 1.1
RED SPRING WHEAT - PRIMARY GRADE DETERMINANTS

Grade Name	Shrunken and Broken			* Degermed	** Grass Green	Pink Kernels	Artificial Stain No Residue	Natural Stain	*** Insect Damage		Dark Immature
	Shrunken	Broken	Total						Sawfly Midge	Grasshopper Army Worm	
No. 1 C.W. Red Spring	6.0%	6.0%	7.0%	4.0%	0.75%	1.5%	Nil	0.5%	2.0%	1.0%	1.0%
No. 2 C.W. Red Spring	10.0%	10.0%	11.0%	7.0%	2.0%	5.0%	5K	2.0%	8.0%	3.0%	2.5%
No. 3 C.W. Red Spring	No Limit	15.0%	No Limit Providing Broken Tolerances Not Exceeded	13.0%	10.0%	10.0%	10K	5.0%	25.0%	8.0%	10.0%
Canada Feed Wheat	No Limit	50.0%		No Limit	No Limit	No Limit	2.0%	No Limit	No Limit	No Limit	No Limit
Final Grade Name	No. 3 C.W. Red Spring	Over 50% grade Sample Broken Grain (notations re kind on request)		Canada Feed Wheat	Canada Feed Wheat	Canada Feed Wheat	Over 2.0% grade Wheat, Sample C.W. Account Stained Kernels (class)	Canada Feed Wheat	Canada Feed Wheat	Canada Feed Wheat	Canada Feed Wheat

*Degermed: Tolerances apply to kernels not classed as sprouted.

**Grass Green Kernels: Tolerances are given as a general guide and may be increased or reduced in the judgment of the inspector after consideration of the overall quality of a sample.

***Insect Damage: Tolerances are not absolute maximums. Inspectors must consider the degree of damage in conjunction with the overall quality of the sample.

Note: The letter "K" in these tables refers to kernel size pieces in 500 grams.

Initially, however, information from the machine vision system is expected to supplement that from other objective tests such as moisture content, protein analyses and test weight in the grading process.

1.2 WHEAT GRADING

1.2.1 Official wheat grading standards

The assignment of grades is made on the basis of sets of standards issued by the Canadian Grain Commission. These are a highly evolved set of guidelines which are authoritatively set forth in the Official Grain Grading Guide of the Canadian Grain Commission. Tables similar to those for Canada Western Hard Red Spring wheat are published for every major class of wheat grown in Canada.

In every case the major quality determinants are the same. These are:

1. the test weight of a standard volume of grain
2. the variety identity
3. the minimum percentage by weight of hard vitreous kernels
4. the degree of soundness
5. absence of foreign material other than wheat
6. absence of wheats of other classes and varieties

In addition to the primary determinants which apply to every sample, grading factors occasionally apply to wheat

which has been adversely affected by a specific condition. These are no less important, however, inasmuch as excessive quantities of any one condition may cause the wheat to be rejected as unsuitable for numerical grading. The "order of precedence" of such factors stated in the OGGG is

> Salvage, Fireburnt, Excreta, Odour, Rotted Kernels, Heated Kernels, Mildewed Kernels, Damaged Kernels, Sprouted Kernels, Dried Kernels, Admixture, Stones

The significance of this order is that the highest ranking of these degradations which is present in excess of a minimum standard appears as part of the official grade of a rejected sample. Machine vision could assist some of these evaluations and play a role as an independent arbiter.

The factors causing a sample to be rejected may be present to a lesser extent in samples eligible for numeric grading. Numeric grades from 1 to 3 in decreasing order of quality are assigned to Hard Red Spring (HRS) wheat. The grade is diminished if admixtures, damaged kernels or other factors exceed the limits set for a particular grade.

1.2.2 Wheat classes and varieties

The wheats grown in Canada are classified on the basis of agronomic, physical and end use characteristics (Bushuk, 1977). While a broad range of wheat classes are grown, the Canada Western Hard Red Spring class and Amber Durums comprise between 80 to 90% and 10 to 20% of the annual volume

of Western Canadian production (Prairie Grain Variety Survey, 1984). Dominant varieties of Hard Red Spring Wheat include Neepawa (52%), Columbus (18%), Benito (5%), Glenlea (2.2%), Sinton (2.0%), Canuck (1.3%) and Leader (1.7%) in decreasing order of production acreage (1984 crop year). The Wakooma, Wascana and Coulter varieties of Durum predominate. Minor classes grown include the Soft White Spring wheats, the Hard Red Winter wheats and semi-dwarf varieties.

1.3 ROLE OF VISUAL PROPERTIES IN THE GRADING OF WHEAT

While a human inspector uses all sensory inputs for evaluation of a wheat sample, most of the necessary information is visual. For this reason, licensed varieties of Hard Red Spring Wheat are bred to be visually indistinguishable in order that wheats of other classes or lesser quality are not confused with them. Quality characteristics such as vitreousness or the discolored states of being "grass-green", "artificially-" or "naturally- stained", "pink" or "dark immature" are by definition visually determined. Many other grading factors, for example, presence of insects, insect damaged or fungus-affected kernels are primarily identified by visual characteristics. Included among the latter are ergot, sclerotinia, mildew, smudge and blackpoint-affected kernels. Visual properties may play roles varying from minor to major in the "key determinants". They are important

for identification of foreign materials, contrasting wheat classes and kernel soundness. Sprouted, shrunken, broken, degermed and "weathered" states are visually identifiable conditions of unsoundness. Conversely, other conditions such as "odour" and "fireburnt" have no visual features.

1.4 APPLICATION OF MACHINE VISION TO WHEAT GRADING

Of the major determinants, it is presently possible to measure test weight in an objective and potentially automatic way.

Machine vision could play a major but as yet largely undetermined role in evaluating the remaining factors. For example, the key property of "vitreousness" which is essentially the light transmission characteristic of wheat kernels is expected to be measurable. This problem may be approached using well-established image processing techniques based on grey levels (pixel light intensity values). Under controlled illumination conditions, the percentage of kernels having a mean intensity value exceeding a specified threshold may be easily counted or mean values of a field of kernels may be computed.

A variety identification method based on the gliadin electrophoregram has been developed recently by Sapirstein and Bushuk (1985). Since the electrophoretic band patterns may be perceived by machine vision and identified us-

ing computers, this procedure could be automated to a great extent.

Any automated process for ascertaining the presence of foreign materials, contrasting wheat classes and unsound kernels is complicated by the large variety of such objects. Arguably, since physical or chemical tests are unlikely to be broadly applicable, precise or rapid enough for this purpose, the image processing and pattern recognition approach seems more attractive.

Previous efforts to measure visual characteristics useful for grading in a potentially automatic way are described in the sections that follow. The use of electro-optical means for perception is common to all this work, but the systems used are remarkably diverse. Initially, the differential reflectance of light of various wavelengths from various grains, i.e. the colour properties, were investigated to determine whether grain identity or wheat vitreousness could be found or measured (Sec. 1.5). Later, the use of grain size characteristics to discriminate among various crops was extensively studied as described in Sec. 1.6. The study of shape characteristics for the same purpose is described in Sec. 1.7. Finally, an overview of past and present research at the University of Manitoba is presented (Sec. 1.8) and the objectives of current research are outlined (Sec. 1.9).

1.5 USE OF LIGHT REFLECTANCE PROPERTIES

Chen, Skarsaune and Watson (1972), using a Hunter Colour Difference Meter, found colour differences between samples of graded wheat and among wheat classes. The colour features used were relative reflectance of blue (435.8 nm), green (546.1 nm) and red (700 nm) light. While no discriminant models nor multivariate tests were applied to the data, the individual colour features used were stated to be insufficient to distinguish between grades. Significantly, however, kernel vitreousness, a major grading factor, and Hunter colour value were found to be correlated.

Hawk, Kauffmann and Watson (1970) used a Beckman DK-2A spectroreflectometer to measure the reflectance from grain samples of infra-red and ultraviolet light in addition to visible frequencies. Each wheat sample tested consisted predominately (95%) of either Hard Red Spring (HRS), Hard Red Winter (HRW), Soft Red Winter (SRW), White or Durum wheats. The complementary portion was made up of a mixture of oats, barley, rye and flax in proportions that reflect expected levels of contamination characteristic of a grade. Ranges of wavelengths within spectral bounds of 420 and 700 nanometers that could maximally discriminate among such samples and others consisting primarily of other cereals, corn or oilseeds were reported. Distinguishing among all samples using such reflectance data was not possible; notable failures of separation were HRS from HRW wheat and barley from oats.

1.6 USE OF KERNEL SIZE CHARACTERISTICS

Edison and Brogan (1972) have presented size measurement statistics of various grains including rye, barley, oats and wheat. Length, width, depth and area data were generated for each kernel. "Plan" and "elevation" views of individual kernels were simultaneously projected onto a viewing screen; length, width and depth measurements were then taken manually with electronic calipers. Area was measured independently using a special apparatus which measured the reduction in light flux received by a photocell obscured by the kernel. High measurement precision was achieved using these techniques.

The distribution parameters presented were similar for the four cereal grains investigated; individual cereals were generally separated by less than 1.25 standard deviations in the four dimensional feature space. Nevertheless, high grain classification accuracies were achieved using a recursive self-learning pattern recognition procedure. This method incorporated "learning" of the class probabilities and classification according to the nearest class mean.

The use of a prototype device for automatic classification of feed grains has been reported by the same workers (Brogan and Edison, 1974).

> The "feature extraction" system operates in the following manner. A sample of a few hundred kernels to be 100% measured is deposited in a conically shaped hopper. A vacuum tube moves into the hopper, picks up a kernel and deposits it in a

> polished groove on a rotating lucite platform. The kernel, oriented with its long axis parallel to the groove, is carried under a 0.5-in. charge-coupled line scanner where plan-form measurements are obtained in digital form with a resolution of about +/-1 ml [sic]. A similar 0.25 in. scanner measures the kernel depth. These measurements are formatted and stored in a buffer and then sent over a telephone link to a remote computer for processing.

Using this apparatus, length, width and depth measurements could be taken rapidly and automatically. A similar system might be developed to present samples for digital image acquisition.

Grain identification based on the nearest class mean rule was unsuccessful; accuracies of greater than 85% for any grain were not achieved. However, when an unsupervised learning approach based on the discrete Kalman filtering algorithm was applied to the same data, accuracies exceeded 98% for all cereal classes.

1.7 USE OF KERNEL SHAPE INFORMATION

Other workers have included at least one shape feature in their investigations of kernel differences. In the earliest study, Segerlind and Weinberg (1972) used shape features exclusively to discriminate among various grains and edible beans. The first ten coefficients of the Fourier transform of the Hough transform of the kernel contour were used as shape features. The kernel image was projected onto a piece of paper having 48 radial lines angularly displaced by 7.5

degrees. Data acquisition was largely manual requiring that the kernel profile be visually centered and then traced by hand. The co-ordinates of intersection of the radial lines with the profile contour were acquired automatically with a digitizer.

The cereals studied included single varieties of rye, white wheat, red wheat, oats, coach oats, 6 row barley and 2 row barley; 50 kernels of each variety were tested. The "nearest class mean rule" operating in a feature space consisting of the 10 harmonics was applied to the training set. The cereal classification accuracies reported were: rye (96%), white wheat (57%), red wheat (93%), oats (71%), coach oats (72%), 6 row barley (84%) and 2 row barley (90%).

While the application of digital image processing to wheat grading is in its infancy, at least two reports of its related use have appeared in the academic literature. Draper and Travis (1984), employing a low cost image analysis system similar to ours, investigated a variety of plant materials which included grains, seeds of weeds and leaves of lettuce. The weeds studied occur as the five most common species contaminating wheat lots in Britain. A single cultivar of wheat ('Avalon') and of barley ('Triumph') were included in the study neither of which is grown in Canada. The metric properties of the objects investigated included area, perimeter, length and width. Length and width were

taken to be equivalent to the sides of the rectangle within which the seed would fit with its long axis parallel to the long side of the rectangle. The two shape factors used were an "aspect ratio" defined to be the ratio of the length to width and the thinness ratio (4π x area / perimeter squared).

The statistical data presented clearly showed that significant differences among the various seeds and grains exist for almost every feature used. No analysis of the discriminatory power of individual features was made nor were the results of optimal classification by linear discriminant functions presented. However, the data suggested that a small number of features and especially aspect and thinness ratios would enable discrimination of wheat from barley.

Certain aspects of the study were unclear. The method of object segmentation from the image background is not stated nor are the discretization or quantization levels of the images. Further, the seed orientations apparent to the viewer, i.e. whether "lateral", "dorsal/ventral" or otherwise, are not described.

Other criticisms of the study are the failure to use the full discriminatory power of the available features using discriminant analysis. Varietal differences in size and shape of wheat and barley were not taken into account. Since the authors were primarily concerned with distinguishing

seeds of weeds from crop species this may not have been necessary.

In an as yet unpublished work (Travis and Draper, 1985), the authors greatly increased the number of species examined. The seeds of seven crop species were examined. The Avalon cultivar of wheat was the only cereal examined and barley was excluded from the study. The seeds of 42 common weeds were included. The same metric properties were used, however, the only shape factor computed was the thinness ratio. Wheat was shown to be well-separated from all other test species in a two-dimensional feature space consisting of thinness ratio and seed length.

Zayas, Pomeranz and Lai (1985) were able to distinguish the wheat cultivar Arkan from Arthur using image analysis. Since the cultivar Arkan has similar morphological characteristics to its Soft Red Winter parent Arthur, their results suggest that fine shape features such as exist between wheat cultivars and classes can be resolved by relatively few shape attributes. Moreover, these features appear to be sufficiently robust for pattern classification since samples from different geographical locations were also accurately classified.

The shape analysis approach taken was more developed than that of the British investigators in the use of a greater number of features and the inclusion of three-dimensional

information. The characteristics of the projections of two orthogonal kernel orientations, crease down and crease right, were measured. Newly introduced features, among others, included a volumetric measurement (the volume of an assumed "equivalent cone") and Feret's diameters representing more "local" information about the kernel contour.

It is not clear how useful these are since neither the canonical discriminant functions nor measurements of the discriminatory powers of the variables , e.g. Wilks' lambda, are presented.

The Feret's diameters are the distances between pairs of parallel tangents to the objects taken at angles differing from each other by 45 degrees. The angles are measured with respect to an arbitrary reference axis which must be identical for each kernel. Therefore, for a typical sound kernel, 8 points on the contour are sampled.

In contrast, all available information about a digitized contour can be represented using Fourier Descriptors (Zahn and Roskies, 1972). There is no need to fix a reference axis or contour starting point since Fourier coefficient magnitudes are invariant to the starting position on the contour used as a reference. Precise alignment of kernels is not required due to the invariance of these values to position or rotation. While Feret's diameters are apparently suitable for objects having very gradual changes of curva-

ture around their perimeter, they may vary considerably for small changes in position of the reference axis for elongated or highly invaginated shapes. The Fourier Descriptors are insensitive to contour energy and are therefore more broadly applicable.

Since the methodology of Zayas et al requires precise orientation and alignment of individual kernels, its potential for automation is low.

1.8 USE OF DIGITAL IMAGE PROCESSING SYSTEMS

In view of the rapid cost reduction and growth of computer-vision hardware and software technology in recent years, their use for wheat grading now seems appropriate. Heretofore, no application of image processing methodologies have been made to this specific problem. In fact, they have rarely been used for the broader problem of grading other grains, oilseeds and vegetable products. Clearly, the methods developed for wheat grading should easily and rapidly extend to these and other problems.

The paucity of previous work contrasts greatly with the wealth of work in biology and medicine. Chromosome analysis, discrimination between and counting of blood cells and classification of cancerous cells (Preston and Onoe, 1976) are all especially well- developed areas of applied work in image processing and pattern recognition. There is fortuitous

similarity between cytological images and those of grains and seeds; for example, a nucleated fibroblast appears much like a germed wheat kernel. Methods developed for such images are likely to be well-suited to the wheat-grading problem.

1.9 UNIVERSITY OF MANITOBA MACHINE VISION RESEARCH

Preliminary work towards developing a machine vision system has been described by Wright (M.Sc. thesis, 1985). An electro- optical imaging system for the purpose of acquiring images of wheat samples was designed. Image arrays of up to 482 by 627 pixels each having 256 levels of intensity registration could be acquired. Major system capabilities include selecting regions within an image, performing thresholding, "zooming" and histogram analysis of such regions, and storing and transferring of image data to main-frame computers for subsequent processing.

In addition, methods for segmentation of images into constituent kernels and for finding structures internal to the kernel such as the germ and crease were developed. Several object perception approaches were taken to the segmentation problem. These included edge detection based on the Haralick (1982) zero-crossing of the second derivative edge operator, use of the Hough transform for detection of elliptical objects and minimum cost function constrained heuristic contour boundary searches. The methods were specially

adapted for kernels that are touching, slightly occluded and/or mutually shadowed.

The features available from monochrome digitized images for the purpose of pattern recognition may be roughly partitioned into gray level, texture, shape and metric (Gonzalez and Wintz, 1977). Each of these categories has been or is being independently studied at the University of Manitoba.

Wright (1985) sought texture features that could discriminate between mature vitreous and unsound kernels having a "shrivelled" or "wrinkled" appearance readily apparent to the untrained viewer. The texture analysis technique used was two dimensional autoregression modelling; the autoregression model parameters characterized the spatial dependence of pixel values. A discriminant model developed using the most discriminatory features achieved correct classifications never exceeding 70% for each category. While it is not clear that the texture analysis approach chosen was optimal, its failure to achieve discrimination between such highly texture-differentiated kernels suggested that texture analysis would not be generally useful in the overall process of wheat grading. Since texture is the primary visual characteristic of kernel soundness and vitrousness, these results were particularly disappointing.

The grey level aspects are undergoing study by Sapirstein (Sapirstein et al, 1985). The intensity of reflected and

transmitted light from individual kernels and kernel aggregates are expected to differentiate among various categories of objects including foreign materials, wheat classes, varieties and possibly grades. Light transmittance is expected to directly measure vitreousness and therefore correlate highly with grade.

Research on shape and metric properties has proceeded in parallel and is the major focus of this thesis.

1.10 ROLE OF SHAPE IN WHEAT GRADING

The intimate relationship between shape analysis and pattern recognition has been the subject of theoretical studies (Pavel, 1983) and much applied work. Attneuve (1954) demonstrated that the information content of shape is concentrated along boundary contours and furthermore at points on these contours at which the direction changes most rapidly. Thus, a general rationale exists for using boundary shapes for recognizing wheat grading elements.

The purpose of the work described in this thesis is to investigate the role that shape and metric features may play in wheat grading. Candidate applications include distinguishing foreign materials such as dockage from wheat, distinguishing other cereals from wheat, distinguishing among various classes of wheat or various species of unsound wheat.

The primary role of shape recognition in wheat grading is expected to be identification of foreign or non-wheat materials. The identification of foreign cereals and discrimination of admixture elements appearing in wheat samples are of importance to most major wheat grading systems of the world (Bushuk, 1977). Foreign materials and wheats of contrasting classes are included among the primary grade determinants of the Canadian system (Official Grain Grading Guide, 1985). Wheats of different classes and varieties are primarily differentiated on the basis of grain morphology (Zayas et al, 1985, Owens and Ainslie, 1971). The kernel profile, be it oval, ovate, or elliptical is a major criterion in cultivar identification (Owens and Ainslie, 1971).

Only the few studies discussed previously relate in any way to distinguishing wheat from potential contaminants using size or shape characteristics. In general, image processing techniques were not used for extracting this information. Shape analysis has been performed on very few varieties most of which are not grown in Canada. In the current work, special attention is paid to varieties of interest to the Canadian wheat grading system.

While wheat grading is the primary concern of this thesis, the separation of other cereals from each other is necessary for their grading, hence this work is more broadly applicable.

Another goal of the research is to ascertain the extent to which shape can differentiate among wheat classes and varieties. In particular, the separation of Hard Red Spring wheats from the Durum species, the utility varieties and other classes of wheat has not been previously attempted. A recent grading problem is that of distinguishing semi-dwarf varieties from established Hard Red Spring varieties. This is presently done on on the basis of the ratio of the germ length to the germ contour length. These are characteristics that may be measured by a machine vision system.

Identification of dockage in wheat samples has not been attempted. The reasons for this are:

1. the samples made available to us have negligible amounts of such material
2. objective measurements of dockage can presently be made using a Carter dockage tester.
3. it has become clear at a very early stage in the research that the highly unusually shaped dockage materials are separable from either wheat or other frequent contaminants.

In relation to soundness, the greater presence of shrivelled and immature kernels in the lower grades should be reflected in smaller kernel perimeters and lesser areas. The separation of damaged kernels such as sprouted, broken or shrunken kernels is expected. These assumptions remain to be verified.

Chapter II

METHODS

2.1 INTRODUCTION

The methods applied to the problems posed for experimental resolution are described in this chapter. Each pattern recognition experiment was conducted in three stages. During the first stage, digital images were acquired and subsequently processed to identify and extract the contours of individual seed images. The image acquisition and segmentation aspects are discussed in Section 2. Next, size and shape characteristics of individual seed images were quantified by methods of contour shape analysis and shape feature description which are the subject of Section 3. Finally, applying the pattern recognition methods overviewed in Section 4, these features were used to develop and evaluate the discriminant model for each "learning problem". In the following chapter, the results of the sequential application of these methods to specific wheat grading problems are described.

2.2 IMAGE PROCESSING OF GRAIN SAMPLE IMAGES

2.2.1 Image Acquisition

Image Acquisition Hardware

Images were acquired using the image acquisition system developed at the University of Manitoba (University of Manitoba Kernel Frame Grabber Manual). The major components of system hardware are a Fairchild CCD3000 digitizing camera under the control of a 80186 based slicer board, a dual 8" disk drive and a display monitor. Image arrays of up to 482 X 627 pixels each having 256 levels of intensity registration may be interactively acquired by an operator issuing commands at a Visual 500 terminal. Subsequent commands are interpreted by the microprocessor to perform windowing, thresholding, histogram analysis and display of images resident in the 256 Kilobytes of on-board memory. Other available software functions include transferring the acquired images to and from 8" floppy disks and the main-frame Data General Eclipse Model MV8000 mainframe upon which most of the subsequent segmentation and shape analysis is performed.

Illumination of samples

For shape analysis, illumination was set up to optimize the contrast between the image object's boundary and its white background. Avoidance of shadow and specular reflection from kernels was desired to facilitate segmentation. These goals were achieved by backlighting the samples in an

otherwise darkened room and providing illumination with a specially modified light box. The light box enclosed a 20.3 cm diameter toroidal lamp (Panasonic F289/CW/RS) located underneath and encircling the sample field. The oblique inwardly directed illumination so obtained minimized the problem of shadows. The top surface of the light box was covered with black cardboard in which a 5.5 cm hole had been cut to allow the oblique passage of light but preventing its direct transmission from lamp to camera. A sheet of opaque white acrylic plastic was placed over the cardboard to diffuse light passing through the aperture. Samples were supported on the plastic surface. The apparatus succeeded in providing backlit, uniform, diffuse, oblique illumination of the field of interest.

Optical adjustments

The digitizing camera was fitted with a Fujinon CCTV CF50B fixed focus lens having a focal ratio of 1:1.4 and a focal length of 50 mm. The focal length was extended by either 10 or 7 mm with Cosmicar Ex-C6 extension tubes depending on the field size desired. Using the 10-mm extension, a 256 by 256 pixel rectangular window centered in the focal plane at a distance of 220 mm from the objective was 21.0 by 21.0 mm. In subsequent sections, images of this size are referred to as "higher resolution" (HR). Otherwise, the field was optimally focussed 305 mm distant from the objective and was 29.0 by 29.0 mm ("lower resolution", LR).

The lens aperture was set at f/2.8 thus achieving optimal contrast between the kernel boundary and background in addition to depth of field sufficient to keep the entire boundary in focus.

The illumination and optical adjustments described performed uniformly over a range of grain samples of different shapes, sizes and opacity.

2.2.2 Segmentation and Encoding

Segmentation of sample images is required in order to extract the thinned simply-connected contours necessary for shape description. A threshold-based isodensity contour follower proved satisfactory for the range of objects tested under the previously described conditions of illumination. The method is an adaptation of the Left-most-looking rule applied to an 8-neighbourhood described in Gonzalez and Wintz (1977) with refinements to cope with "unusual" geometries. Contours were encoded according to Freeman's method (1961) which, in essence, sequentially encodes the tangent angle at successive points along a quantized curve (Bennett and MacDonald, 1975). The contour-position functions described by Tang (1981) enabled rapid regionfilling.

Segmentation of images into image constituents was greatly simplified because:

1. the background was completely untextured
2. the foreground objects were non-occluded;
3. contrast beween object boundary and background was maximized.

Segmentation produces a chain-encoded representation of an object's shape that may be further analyzed by methods described in the following section.

2.3 SHAPE DESCRIPTION AND ANALYSIS

2.3.1 Introduction

The central problem of shape description is to represent a shape or provide shape information in a mathematical form appropriate to pattern recognition techniques. Major methods of shape representation are reviewed in this section. The most fundamental of these, employing a curvature function, is described in 2.3.2; the Freeman chain code is a form of discrete curvature representation. Sampling aspects of the discrete representation of shape are also discussed in the context of curvature representation. In the subsections that follow, three classical methods used for pattern recognition, namely, normalized shape moments (2.3.3), moment invariant functions (2.3.4) and Fourier descriptors (2.3.5) are described. Finally, descriptors of shape attributes are discussed (2.3.6).

2.3.2 Curvature representation

Because of the salient role that curvature and particularly points of maximum absolute curvature appear to have in shape recognition and understanding (Attneuve, 1954), representation by some curvature function seems logical. For the simple continuous closed contour shown in Fig. 2.1, the shape may be described by specifying its curvature as a function of arc length. The contour curvature ,$\kappa(s)$, is defined as the rate of change of the angle ϕ with respect to the arc length s, i.e.

$$\kappa(s) = \frac{d\phi}{ds} \qquad 2.1$$

where ϕ is the angle between the tangent of the curve and the positive x-direction. Some geometric sense of the meaning of the curvature function may be had by considering the radius of curvature, $1/\kappa(s)$, of a circle normal to the arc tangent. The arc is concave on the left if $\kappa(s)>0$ as s increases in the counter-clockwise direction. The curvature function is periodic in s having a period equal to the perimeter length (S) of the closed contour. The shape can be reconstructed by finding its rectangular coordinates from

$$x(s) = \int_0^s \cos\left(\int_0^\alpha \kappa(\lambda)d\lambda + \phi_0 \right) d\alpha + x(0) \qquad 2.2$$

$$y(s) = \int_0^s \sin\left(\int_0^\alpha \kappa(\lambda)d\lambda + \phi_0 \right) d\alpha + y(0) \qquad 2.3$$

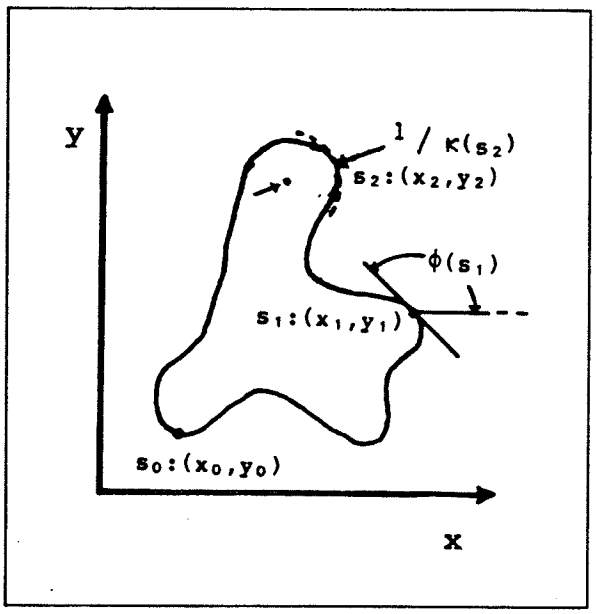

Fig. 2.1 Contour Curvature

where x(0) and y(0) are starting co-ordinates.

For curvature functions defined on discrete image arrays the tangent angle and curvature become

$$\phi(s_j) = \tan^{-1} \frac{y(s_j) - y(s_{j-1})}{x(s_j) - x(s_{j-1})} \quad , \qquad 2.4$$

$$\kappa(s_j) = \phi(s_j) - \phi(s_{j-1}) \quad . \qquad 2.5$$

The Freeman chain code is a special case of the above where $\phi(s_j)$ is allowed to take on one of eight values $\pi/4$ radians apart. Such discrete shape representations are produced from samples of an underlying continuous shape acquired by the image sensing elements.

The fidelity of the discrete representation, i.e. the Freeman chain code, depends on the image sampling frequency. The requisite frequency may be easily related to curvature representation requirements. The sampling intervals must be fine enough in order that the high curvature characteristic of the boundary detail be represented. Implicitly, a subjective decision as to what boundary detail is significant must be made. For most objects found in wheat samples, the most important information resides towards the ends.

The problem of accurately representing the curvature at every point of a sampled closed curve of, for example, a wheat kernel was addressed by Young (1974). If such a curve has a point of maximum curvature K_m, then, the sampling increments of arc length must satisfy

$$\Delta s < \pi / 2 K_m \quad . \qquad 2.6$$

This especially pertains to distinguishing rounded, pointed or blunt ends which tend to characterize wheat and like kernels. Quantization error, inherent to discrete representation, affects curvature and the mathematical descriptions that follow.

While intuitively appealing and conceptually useful, problems associated with the curvature representation limit its use for pattern recognition studies. One difficulty is that if a shape has sharp corners, the curvature function is undefined at these points. Zahn and Roskies (1972) proposed the use of a cumulative curvature function defined as

$$\theta(s) = \int_0^s \kappa(\alpha)d\alpha - \frac{2\pi s}{S} \qquad 2.7$$

to overcome this problem.

Another inconvenience is that suitable features for pattern recognition must be developed from the representation which is not, unlike following mathematical descriptions, in a form immediately usable for statistical pattern recognition. The Fourier Descriptor and Moment methodologies are appropriate to distinguish subtle differences between shapes (Pavladis, 1978) such as exist between wheat kernels. These techniques are described in the sections that follow.

2.3.3 Shape Moment Representation

Two variants of the method of moments which are invariant to size, position and rotation have been described in the literature. In one method, the principal axes of the image are determined and the moments are transformed to align with these axes. Reeves and Rostampour (1981) describe the principal axis method in relation to the task of identifying segmented objects in aerial photographs.

The second method consists of generating a set of simple combinations of moments called moment invariants which are algebraically invariant to positional change. Hu (1962) describes seven such functions derived from moments up to order three. The finding of principal axes is not necessary

for their evaluation. This method has been used for aircraft identification (Dudani et al, 1977) and scene matching (Wong, 1978).

2.3.3.1 Moment Method 1: Principal-axis Method

The basis of this method is the discrete computation of the image moment defined as

$$M(u,v) = \int_{(x,y)\ \epsilon R} \int f(x,y)\ x^u y^v dxdy \quad . \qquad 2.8$$

The function f(x,y) may represent binary or grey-level images (Reeves and Rostampour, 1981). In the latter case, the moments depend on the grey level distribution interior to the contour as well as the contour shape. In future, such gray-level moments may be useful for describing the visual "texture" of image contituents. However, only binary images are considered in this thesis; the derived moments are dependent only on contour shape.

In the discrete case, the moment M_{pq} of a digital image is defined by

$$M_{pq} = \sum_x \sum_y x^p y^q f(x,y) \qquad 2.9$$

where x and y are integer-valued pixel co-ordinates. The image function , f(x,y), is unity on and within the object's contour and zero otherwise. The set of moments $\{M_{pq}\}$,p,q=0,1,2..is uniquely defined by f(x,y) and conversely f(x,y) is uniquely determined by $\{M_{pq}\}$. The moments with respect to the image co-ordinate axes x and y up to the order (p+q) of interest are first computed. A series of normalization procedures such as described by Reeves (1981) are performed to generate size, orientation and position-invariant quantities.

First, all moments are referred to an object's centroid in order to translationally normalize them. The position of the centroid ($\bar{x},\bar{y}$) of the object may be determined from the object's area (M_{00}) and first order moments:

$$\bar{x} = M_{10}/M_{00} \qquad 2.10$$

$$\bar{y} = M_{01}/M_{00} \quad . \qquad 2.11$$

The central moments which are invariant to translations of the object are defined by

$$\mu_{pq} = \sum_x \sum_y (x-x)^p (y-y)^q f(x,y) \qquad 2.12$$

They may be rapidly computed from the original moments using

$$\mu_{pq} = \sum_{r=0}^{p} \sum_{s=0}^{q} C(p,r)\ C(q,s)\ (-1)^{r+s}\ M_{p-r,q-s} \qquad 2.13$$

where

$$C(p,r) = \frac{p!}{r!\ (p-r)!} \quad . \qquad 2.14$$

The rotational normalization procedure refers all moments to the major principal axis of the object being analyzed. The angle θ from the original x-axis to the principal axis of the object (Fig. 2.2) satisfies

$$\tan(2\theta) = 2\mu_{11}/(\mu_{20}-\mu_{02}) \quad . \qquad 2.15$$

The rotationally normalized moments may be computed from

$$\phi_{pq} = \sum_{r=0}^{p} \sum_{s=0}^{q} (-1)^{q-s} C(p,r)C(q,s)(\cos\theta)^{p-r+s}(\sin\theta)^{q-s}\mu_{p-r+q-s,r+s} \qquad 2.16$$

When the object is m-fold symmetric, θ is not unique and there are multiple possible sets of principal axes. By convention, a unique principal axis is chosen by requiring that

1. $\phi_{20} > \phi_{02}$

2. $\phi_{03} > 0$.

The correct rotation angle

$$\theta^{*} = \theta + n\pi/2 \qquad 2.17$$

substituted into the above expression will satisfy these constraints and produce the correct rotationally normalized moments.

Size normalization is achieved by employing the following transformation:

$$n_{pq} = \phi_{pq}/\phi_{oo}^{\lambda} \qquad 2.18$$

where

$$\lambda = (p+q)/2 + 1 \quad . \qquad 2.19$$

The moment measures obtained are physically interpretable; the moment sequences $\{\bar{n}_{p0}\}$ and $\{n_{0p}\}$, p=1,2..are the moments of a projection of the object along the minor and major axes onto the x' and y' axes (Fig 2.2) respectively.

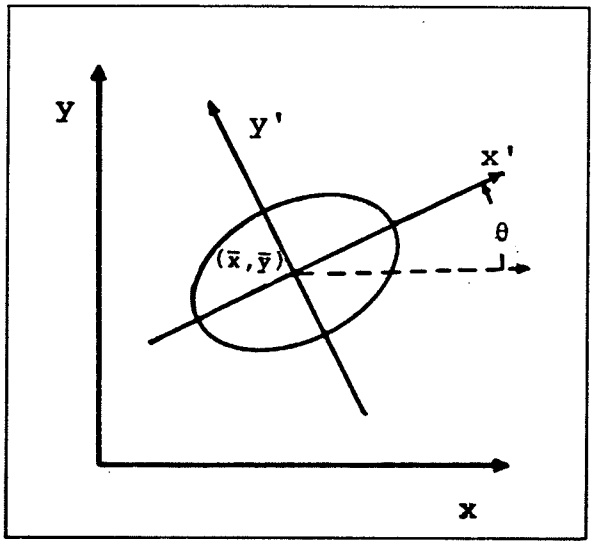

Fig. 2.2 Co-ordinate System Transformation

Moments referred to x'-y' system

2.3.3.2 Rapid Computation of Moments

A rapid method for the computation of object moments based on the discrete implementation of Green's theorem is described in Tang (1981).

Green's theorem in the continuous x-y plane states that

$$\int\int_R \left(\frac{\partial g}{\partial x} - \frac{\partial f}{\partial y}\right) dxdy = \int_C fdy + gdx \qquad 2.20$$

where C is a boundary consisting of piecewise smooth simple closed curves and f(x,y) and g(x,y) are continuously differentiable functions defined in a region containing R and C. When g=0, this equation simplifies to

$$\int\int_R \frac{\partial f}{\partial y} dxdy = \int_C fdy \quad . \qquad 2.21$$

Tang shows how this expression can be computed over R, a discrete 8-connected region without holes in the subspace

$$S' = \{ (h,k),\ h>0,\ k>0\ ,\ h,k\text{:integers} \}$$

having a boundary expressed as an l-element chain code:

$$B: \{ (x_0,y_0),\ a_0,\ a_1 \ \ldots\ a_{l-1} \}.$$

A summation over the sequential boundary is performed; the contour position functions C_y and D_y (Table 2.1, page 37) are computed for each boundary element to calculate the element's contribution to the summation. In discrete form the expression becomes

$$\sum_{m,n\epsilon R} f(m,n) = \sum_{i=0}^{l-1} F_x(x_i,y_i)D_y(a_{i-1},a_i)+f(x_i,y_i)C_y(a_{i-1},a_i) \qquad 2.22$$

where

$$F_x(x_i,y_i) = \sum_{j=0}^{x_i} x_j{}^{u} y_i{}^{v} \quad . \qquad 2.23$$

and

$$x_{i+1} = x_i + a_i x_i \qquad 2.24$$

$$y_{i+1} = y_i + a_i y_i \quad . \qquad 2.25$$

The uv-th moment of the region R is defined as

$$M_{uv} = \sum_{(m,n)\epsilon R} m^{u} n^{v} \qquad 2.26$$

where (m,n) is the co-ordinate of any point in R. If R is in chain-encoded form then the moments may generally be computed from

$$M_{uv} = \sum_{i=0}^{l-1} F_x(x_i,y_i)D_y(a_{i-1},a_i) + f(x_i,y_i)C_y(a_{i-1},a_i) \qquad 2.27$$

where $F_x(x_i, y_i)$ in this case is

$$F_x(x_i, y_i) = \sum_{j=0}^{x_i} f(x_j, y_i) \qquad 2.28$$

If the moment-defining relationship is used to compute the moments, the number of computations is proportional to M_{00} (i.e. the area) whereas if the discrete method is used, the number of computations is proportional to the length of the sequential boundary which is related to $\sqrt{M_{00}}$.

Table 2.1

Contour Position Functions

$D_y(a_{i-1}, a_i)$

a_{i-1} \ a_i	1	2	3	4	5	6	7	8
1	0	1	1	1	1	0	0	0
2	0	1	1	1	1	0	0	0
3	0	1	1	1	1	0	0	0
4	0	1	1	1	1	0	0	0
5	-1	0	0	0	0	-1	-1	-1
6	-1	0	0	0	0	-1	-1	-1
7	-1	0	0	0	0	-1	-1	-1
8	-1	0	0	0	0	-1	-1	-1

$C_y(a_{i-1}, a_i)$

a_{i-1} \ a_i	1	2	3	4	5	6	7	8
1	0	0	0	0	0	0	0	0
2	0	0	0	0	0	1	0	0
3	0	0	0	0	0	1	1	0
4	0	0	0	0	0	1	1	1
5	1	0	0	0	0	1	1	1
6	1	1	0	0	0	1	1	1
7	1	1	1	0	0	1	1	1
8	1	1	1	1	0	1	1	1

2.3.4 Moment Method 2: Moment Invariant Functions

The central moments defined previously may be normalized with respect to size and combined to determine functions which are also invariant to positional, rotational and size change. These are abstract quantities which are not geometrically interpretable. The moment invariants derived by Hu (1962) are listed below.

$$M_1 = (\mu_{20}+\mu_{02}) \qquad 2.29$$

$$M_2 = (\mu_{20}-\mu_{02})^2+4\mu_{11}^2 \qquad 2.30$$

$$M_3 = (\mu_{30}-3\mu_{12})^2+(3\mu_{21}-\mu_{03})^2 \qquad 2.31$$

$$M_4 = (\mu_{30}+\mu_{12})^2+(\mu_{21}+\mu_{03})^2 \qquad 2.32$$

$$M_5 = (\mu_{30}-3\mu_{12})^2(\mu_{30}+\mu_{12})[(\mu_{30}+\mu_{12})^2-3(\mu_{21}+\mu_{03})^2] + (3\mu_{21}-\mu_{03})(\mu_{21}+\mu_{03})[3(\mu_{30}+\mu_{12})^2-(\mu_{21}+\mu_{03})^2] \qquad 2.33$$

$$M_6 = (\mu_{20}-\mu_{02})[(\mu_{30}+\mu_{12})^2-(\mu_{21}+\mu_{03})^2] + 4\mu_{11}(\mu_{30}+\mu_{12})(\mu_{21}+\mu_{03}) \qquad 2.34$$

$$M_7 = (3\mu_{21}-\mu_{03})(\mu_{30}+\mu_{12})[(\mu_{30}+\mu_{12})^2-3(\mu_{21}+\mu_{03})^2] - (\mu_{30}-3\mu_{12})(\mu_{21}+\mu_{03})[3(\mu_{30}+\mu_{21})^2-(\mu_{21}+\mu_{03})^2] \qquad 2.35$$

Size normalization of central moments is again accomplished by division of a particular moment by an appropriate power of μ_{00} (Wong, 1978)

$$\mu_{pq}^{*} = \frac{\mu_{pq}}{\mu_{00}^{\lambda}} \quad , \qquad 2.36$$

$$\lambda = \frac{p+q}{2} \quad . \qquad 2.37$$

2.3.5 Fourier Descriptor Representation

The theoretical basis of this method is discussed by Zahn and Roskies (1972). An object may be viewed as being in the complex plane in which the points (x,y) on the contour of the object become the complex numbers x + iy. A sequence of complex numbers is generated by traversing the contour in a counterclockwise direction and sampling it at intervals of arc length. The boundary function described in this way is periodic and may alternately be expressed as its Fourier transform. The Fourier descriptor is defined as the discrete Fourier transform of the complex number sequence.

The procedures required to normalize the representation follow from the properties of the transform. By linearity, if the size of the contour is changed by multiplying the descriptor components by a constant, then the contour co-ordinates are multiplied by the same constant. Rotation of the contour by angle θ is achieved by multiplying the coefficients by $\exp(j\theta)$. The contour starting point may be shifted by multiplying the k-th frequency component in the frequency domain by $\exp(jkt)$ where t is the fraction of the period 2π .

The normalized representation is invariant to object size, orientation and position within the image and the starting point on the contour. Standardization of size is achieved by the division of all components by the magnitude

of the first Fourier harmonic. Position invariance naturally results from referring the description to some point on the contour itself. The orientation and starting point normalizations require a phase transformation of the Fourier descriptor and leave component magnitudes unchanged. Therefore, to reconstruct a shape in its original orientation referred to its correct starting point, the descriptor phase information must be known. If, as for the work in this thesis, such reconstruction is unnecessary, then the phase information can be ignored. The set of size-normalized component magnitudes are sufficient to uniquely describe a given shape and will be invariant to rotation, position and starting point.

The major problems associated with the Fourier Descriptor method are avoided by neglecting the orientation-starting point normalization. One difficulty is that the procedure is performed according to a complicated set of rules (described by Zahn and Roskies (1972)) which add greatly to the required computation. Also, this procedure, being dependent on selection of harmonics having the largest magnitude, is sensitive to quantization noise.

In addition to problems inherent to the Fourier Descriptor method are the inconveniences of the original technique used by Zahn and Roskies. Their method required the entry of the coordinates of 2^n (n an integer) equally-spaced samples of a continuous contour. In contrast, a method

which is both computationally simpler and adapted to variable length Freeman-encoded contours such as are extracted from digital images is described by Chuan-Juan and Quing-Yun (1980). Their procedure is outlined below.

The boundary contour C of a segmented object can be represented by a complex-valued function:

$$u(t) = x(t) + jy(t), \quad 0 \leq t \leq 2\pi \tag{2.38}$$

where x(t) and y(t) are co-ordinates of a point Q on the contour.

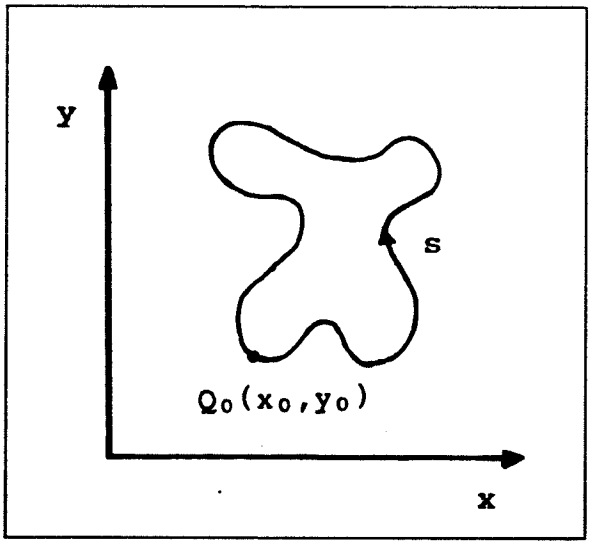

The normalized arc length of Q from the contour starting point $Q_0(x_0,y_0)$ is

$$t = 2\pi s/S \tag{2.39}$$

where s is the arc length measured in the counterclockwise direction from Q_0 and S is the contour perimeter length.

Since u is periodic in t, it can be expressed as a Fourier series of the form

$$u(t) = \sum_{n=-\infty}^{\infty} P_n e^{jnt}, \quad 0 \leq t \leq 2\pi \qquad 2.40$$

having Fourier coefficients

$$P_n = \frac{1}{2\pi} \int_0^{2\pi} u(t)\, e^{-jnt} dt, \quad n = 0, \pm 1, \pm 2, \ldots \; . \qquad 2.41$$

The n-th coefficient ($n \neq 0$) may be approximately computed from the contour chain code using

$$P_n = \frac{1}{2n\pi j} \sum_{m=1}^{M} a_m e^{j(\frac{\pi}{4} q_m - 2n\pi \sum_{k=1}^{m} a_k / \sum_{k=1}^{M} a_k)}, \quad n = \pm 1, \pm 2, \ldots \qquad 2.42$$

where q_m denotes the m-th component of an M-length chain code and

$$a_k = \begin{cases} 1 & \text{if } q_k \text{ is even} \\ \sqrt{2} & \text{if } q_k \text{ is odd} \end{cases} \; . \qquad 2.43$$

The coefficient P_0 representing the position of the shape centroid may be calculated from

$$P_o = u_o - \sum_{m=2}^{M} a_m e^{j(\pi/4)q_m\left(\sum_{k=1}^{m-1} a_k \,/\, \sum_{k=1}^{M} a_k\right)} \qquad 2.44$$

where $u_0=u(0)=x(0)+y(0)$. The other coefficients are abstract quantities.

As previously stated, Fourier coefficient magnitudes may be used as pattern recognition features. The range of harmonics useful for this purpose must be determined. Also, various important geometric properties of a contour e.g. roundness, curvature and elongation, may be computed as summations of functions of Fourier coefficients. It is therefore important to consider bandwidth, series convergence and truncation effects on their computation.

The highest harmonic that can be considered for any purpose is $\mathrm{mod}(n_1,2)$ where n_1 is the length of the shortest chain code representing a contour. In fact, the useful bandwidth is much less, being restricted by noise which dominates at high frequencies. This effect is a consequence of the emphasis of quantization noise at high frequencies by the linear transfer function magnitude of the differentiation operations necessary to compute the tangent angle and curvature.

> The problem is exacerbated by the non-linear process of both curvature and tangent angle function measurement which amplifies the high frequency quantization noise components on the quantized shape boundaries and to some extent distribute this quantization noise over the entire spectral range of the one-dimensional functions.
> (Bennett and MacDonald, 1975).

The $n_1/4$-th harmonic is the highest that may be considered unaffected by noise. According to Bennett and MacDonald (1975), the range of harmonics that contribute to shape discrimination is even narrower. They related the highest harmonic, Hu, useful for this purpose to the number of significant points, P, of high convex curvature of the shape, stating, as a general rule:

$$H_u < 3P \text{ to } 4P \quad . \qquad 2.45$$

Observing this guideline, the first ten harmonics have generally been computed for the objects studied in this thesis.

2.3.6 Other Descriptors

In the previous sections, "information-preserving" (Pavladis, 1978) descriptions of shape have been outlined. Such representations enable complete reconstruction of the shape within the limits of discretization error. In the sections that follow, descriptors of specific size and shape characteristics are outlined. Frequently such attributes may be computed as functions of moments or Fourier descriptors.

2.3.6.1 Size Properties

a. Perimeter Length

The contour length may be approximated in the discrete case by

$$S \approx \sum_{k=1}^{M} a_k \qquad 2.46$$

where, as before

$$a_k = \begin{cases} 1 \text{ if } q_k \text{ is even} \\ \sqrt{2} \text{ if } q_k \text{ is odd} \end{cases} . \qquad 2.47$$

b. Contour Area

A rapid method for computing the contour area of a Freeman chain-encoded contour is based on the discrete calculation of the expression

$$\int\int_R dxdy = \int_C xdy = \text{Area} \qquad 2.48$$

derived from Green's theorem. As before, R is the region enclosed by and including the contour C. In the discrete region R having boundary B described in Section 2.3.2 the area is

$$\text{Area} = M_{oo} = \sum_{i=0}^{l-1} x_i D_y (a_{i-1}, a_i) + C_y(a_{i-1}, a_i) \qquad 2.49$$

where C_Y and D_Y are the contour position functions described previously.

c. Minimum Enclosing Rectangle: Length, Width

These dimensions represent the length and width of the minimal enclosing rectangle (MER) of the contour. A translational and rotational transformation is first applied to the contour co-ordinates such that the origin of the new co-ordinate system is located at the centroid and the object's major principal axis becomes the x-axis while the minor principal axis maps into the ordinate axis. The transformation necessary to accomplish this is

$$\begin{bmatrix} x' \\ y' \end{bmatrix} = \begin{bmatrix} \cos\theta & -\sin\theta \\ \sin\theta & -\cos\theta \end{bmatrix} \begin{bmatrix} x-h \\ y-k \end{bmatrix} \qquad 2.50$$

where θ is found as in Section 2.3.3.1 ~~2.3.1b.~~ The transformed contour co-ordinates form M-element sets $\{ x_k' \}$ and $\{ y_k' \}$. The MER has length

$$L = \max_{k=1,M} \{x_k'\} - \min_{k=1,M} \{x_k'\} \qquad 2.51$$

and width

$$W = \max_{k=1,M} \{y_k'\} - \min_{k=1,M} (y_k') \quad . \qquad 2.52$$

2.3.6.2 Elongation Measurements

In previous investigations (Draper and Travis, 1984, Travis and Draper, 1984) elongation measurements were shown to be powerful discriminatory features. One ubiquitous measure is the thinness ratio defined by

$$T = 4\pi(A/p^2) \qquad 2.53$$

where A is the figure area and p is the perimeter length. The more elongated the figure is, the closer the thinness ratio will be to zero.

Aspect ratio is a second property that can be used to measure the elongation of a figure. One definition is the ratio of length to width of the MER. The sides of the MER are parallel to the eigenvectors of the binary image function. The eigenvectors physically correspond to the directions about which the figure has maximum and minimum moments of inertia; the corresponding eigenvalues are the two moments of inertia. The ratio of the larger to smaller eigenvalue defines a second aspect ratio. Tang (1981) gives this as:

$$A = \max(\alpha,\beta)/\min(\alpha,\beta) \qquad 2.54$$

where α and β are eigenvalues of the matrix

$$\begin{bmatrix} C_{20} & C_{11} \\ C_{11} & C_{02} \end{bmatrix}$$

and

$$c_{20} = \frac{M_{20}}{M_{00}} - \left(\frac{M_{10}}{M_{00}}\right)^2 \qquad 2.55$$

$$c_{02} = \frac{M_{02}}{M_{00}} - \left(\frac{M_{01}}{M_{00}}\right)^2 \qquad 2.56$$

$$c_{11} = \frac{M_{11}}{M_{00}} - \frac{M_{01}}{M_{00}} \times \frac{M_{10}}{M_{00}} \quad . \qquad 2.57$$

2.3.6.3 Energy

The occasional appearance of "unusually-shaped" objects in wheat sample images may be expected. Such objects, for example insects, generally have more complex shapes than those of wheat or other cereals. Their rapid screening, without complete shape description being necessary, might be achieved using a "complexity" feature.

Several curvature-based features are correlated with the psychological perception of boundary complexity. These include the circularity measurement P^2/A, the number of changes of sign of the curvature function along the boundary and measurements of convex deficiency. Young (1974) describes the concept of boundary energy in analogy with bending energy in elasticity theory. The average energy per unit length of a simply-connected closed contour is given by

$$E = \frac{1}{S}\int_{0}^{S} |\kappa(s)|^{2} ds \quad . \qquad 2.58$$

The discrete equivalent described by Young was implemented.

2.3.6.4 Symmetry

Many of the objects of interest in wheat sample images are bilaterally symmetric, e.g. wheat is elliptical. Certain objects such as broken kernels might be detected by abnormal asymmetry about one axis. The moments n_{0q} and n_{p0} represent the statistical moments of the projection of the object on to one of the principal axes. The projection may be thought of as a statistical distribution. The usual parameters that describe such a distribution are

$$\text{variance} = n_{20} \qquad 2.59$$

$$\text{skewness} = n_{30}/n_{20}^{3/2} \qquad 2.60$$

$$\text{kurtosis} = n_{40}/n_{20}^{2} - 3 \quad . \qquad 2.61$$

Abnormal asymmetry is reflected in high values of skewness. Similarly, parameters for the other axis can be obtained.

2.3.6.5 Ellipse Fitting

The elliptical characteristics of certain wheat varieties differentiates them from other varieties and cereals (Owen and Ainslie, 1971). Therefore, the two parameters which

describe an elliptical shape, i.e. lengths of the semi-major and semi-minor axes may be useful for this purpose.

An ellipse of general form

$$a_1x^2 + a_2x + a_3y^2 + a_4y + a_5xy - 1 = 0 \qquad 2.62$$

may be fitted to a contour in the least-squared-error sense. The solution is given by

$$\underline{a} = S^{-1}\underline{b} \qquad 2.63$$

where S is the symmetric matrix

$$S = \sum_{i=1}^{cl} \begin{bmatrix} x_i^4 & x_i^3 & x_i^2y_i^2 & x_i^2y_i & x_i^3y_i \\ x_i^3 & x_i^2 & x_iy_i^2 & x_iy_i & x_i^2y_i \\ x_i^2y_i^2 & x_iy_i^2 & y_i^4 & y_i^3 & x_iy_i^3 \\ x_i^2y_i & x_iy_i & y_i^3 & y_i^2 & x_iy_i^2 \\ x_i^3y_i & x_i^2y_i & x_iy_i^3 & x_iy_i^2 & x_i^2y_i^2 \end{bmatrix} \qquad 2.64$$

and $b^T = (\Sigma x_i^2\ \Sigma x_i\ \Sigma y_i^2\ \Sigma y_i\ \Sigma x_iy_i)$. The subscript denotes the i-th element of the contour and summation is taken over all such elements.

A measure of deviation from the elliptical shape is the mean- squared error defined as

$$E_{RMS} = \sqrt{S_E^2/cl} \quad . \qquad 2.65$$

The total squared error of the ellipse fit is given by

$$S_E^2 = \sum_{j=1}^{cl} (a_1 x_i^2 + a_2 x_i + a_3 y_i^2 + a_4 y_i + a_5 x_i y_i - 1)^2 \quad . \qquad 2.66$$

The fractional difference in area between a contour and its fitted ellipse is another useful indicator of deviation from elliptical shape.

2.4 PATTERN RECOGNITION ASPECTS

2.4.1 Linear Discriminant Analysis

Single stage classifiers have been applied to the problems of supervised learning described in the following chapter. The average probability of sample misclassification is minimized by the Bayes classifier approach. Bayes discriminant functions of the form

$$d_i(\tilde{x}) = \tilde{w}_i^T \tilde{x} \qquad 2.67$$

were developed from the training data where $\tilde{x}$ represents a set of features $\{ x_j \}$, $j = 1, 2, \ldots d$ in a d-dimensional feature space X and i denotes one of the M classes among which discrimination is sought. The state conditional probability density functions describing individual features are assumed to be normal, i.e.

$$p(x_j | \omega_i) = \frac{1}{\sqrt{2\pi}} \sigma_i e^{-(x_j - \mu_i)/2\sigma_i^2} = N(m_i, \sigma_i) \quad . \qquad 2.68$$

A posteriori probabilities of class membership are given by

$$P(\omega_i|\,\tilde{x}) = \frac{Pr(\omega_i)\; P(\tilde{x})|\,\omega_i)}{\sum_{i=1}^{M} Pr(\omega_i)p(\tilde{x}|\,\omega_i)} \quad . \qquad 2.69$$

Samples are classified into the group having the highest a posteriori probability of correct classification. The squared Mahalanobis distance between class mean vectors

$$r^2 = (\mu_2 - \mu_1)^T C_1^{-1} (\mu_2 - \mu_1) \qquad 2.70$$

is a convenient measure of class separation.

2.4.2 Stepwise Discriminant Analysis

Choice of appropriate classification variables may be assisted by stepwise discriminant analysis (SAS, 1982). The discriminatory power of a set of features as measured by Wilks' lambda (Tatsuoka, 1970) is the basis for this analysis.

Letting $S_W(\tilde{x})$ denote the Within-Class Scatter Matrix for variables $\tilde{x} = (x_1, x_2, \ldots x_p)$, $p<d$ and $S_T(\tilde{x})$ the total generalized dispersion for the same set of variables, then Wilks' lambda

$$\Lambda(\tilde{x}) = \frac{\det|\, S_W(\tilde{x})|}{\det|\, S_T(\tilde{x})|} \qquad 2.71$$

indicates the group separation capacity of $\tilde{x}$.

Variables enter the discriminant model in order of the magnitude of the change of $\Lambda(\tilde{x})$ due to the addition of that variable. The F-statistic is used to test the significance of the change in $\Lambda(\tilde{x})$. Only features exceeding an F threshold are allowed to enter and remain in the discriminant model. An F-test significance level of 15% was chosen as the threshold for entry or removal of a variable.

Chapter III

RESULTS AND DISCUSSION

3.1 INTRODUCTION

The role that size and shape features described in the previous chapter can play in various wheat grading problems is presented in this chapter. In particular, their capacity to identify the technical categories of foreign materials, admixture cereals, wheats of other classes, wheat and other cereal varieties are discussed. These problems have been posed for resolution in increasing order of difficulty of the recognition task. The major shape description methodologies were compared in relation to their cereal discrimination capacity. Finally, discernment of damaged or unsound wheat species from sound mature wheat species was attempted. Experimental materials referred to throughout the chapter are described in the following section.

3.2 MATERIALS

Samples of dockage-free, pedigree cereal seed were obtained from United Grain Growers of Winnipeg and the Alberta Wheat Pool. A broad set of wheat cultivars were provided from seed stocks maintained by the Plant Science Department

Table 3.1

Crop species chosen for investigation

SEED CATEGORY	SPECIES/CULTIVAR
CANADA WESTERN RED SPRING WHEAT	WHEAT (TRITICUM aestivum L.) 'Neepawa' 'Columbus' 'Benito' 'Katepwa' 'Glenlea' 'Park'
HARD RED WINTER WHEAT	WHEAT (TRITICUM aestivum L.) 'Norstar'
SOFT WHITE SPRING WHEAT	WHEAT (TRITICUM aestivum L.) 'Owens' 'Fielder'
UTILITY WHEAT	WHEAT (TRITICUM aestivum L.) 'Glenlea' Hy320
AMBER DURUM WHEAT	WHEAT (TRITICUM durum L.) 'Arcola' 'Coulter' 'Wakooma' 'Wascana'
ADMIXTURE CEREALS	RYE (SECALE Cereale) 'Muskateer' 'Puma' 'Gazelle' BARLEY (HORDEUM vulgare L.) 'Johnston' 'Bonanza' 'Klages' OATS (AVENA Sativa) 'Fidler' 'Harmon'
ADMIXTURE OILSEEDS	CANOLA (BRASSICA napus, L.)
WEED SEEDS	WILD OATS (AVENA fatua, L.)

tically, the sprouts had barely emerged (between 1 and 2 mm) from the germ end. Only those showing this early stage of germination were selected.

3.3 DISCRIMINATION BETWEEN WHEAT AND FOREIGN MATERIALS

Foreign materials are defined to be objects other than wheat which appear in samples following cleaning. Clearly there are many such objects. The investigation was therefore restricted to

a) those most frequently occurring and/or

b) those which are defined by statute to be contaminants.

The category of foreign materials is further dichotomized into the sub-categories of cereal grains and materials other than cereal grains (Table 1.1, page 2-3).

The extraneous matter includes dockage materials that would ordinarily be removed by cleaning. Examples of this group are wheat heads, husks, loose sprouts, straw and other air liftings and small seeds, wild oats and stones (Bushuk, 1977) with stones counted apart from other objects. Also included are an unlimited set of objects which may not necessarily be anticipated in a wheat sample.

While dissimilar to wheat and other cereals, such alien objects are generally non-uniform in size and shape; the visual characteristics that distinguish them are their asymmetry and "complexity". In the final system realization,

of the University of Manitoba in addition to the above sources. Wheat variety identities were verified by gliadin electrophoregram (Sapirstein and Bushuk, 1985).

Cultivars were chosen from the following categories of grains:

a. Hard Red Spring Wheat (HRS)
b. Hard Red Winter Wheat (HRW)
c. Soft White Spring Wheat (SWS)
d. Utility Wheat.
e. Durum Wheat

Classes a. to d. are referred to as Common Wheats to distinguish them from the Durum species.

Samples of graded wheats were obtained from the Grain Inspection Division of the Canadian Grain Commission. Miscellaneous samples, including wild Oats and Canola, were provided by a local grower. Crop species and cultivars chosen for investigation are summarized in Table 3.1.

Samples of "unsound" wheat were obtained from the Plant Science Department of the University of Manitoba. These included the "broken", "shrunken" and "sound mature" wheat categories. The sprouted kernels were developed by germination of "sound" kernels. Samples were placed in Petri dishes on dampened filter paper and stored at 4 degrees Centigrade for 12 hours in the dark. They were then incubated for 48 hours at room temperature in sunlight. Characteris-

such foreign material may be operationally defined as materials which do not fall into the remaining identifiable classes of wheats, cereals, etc. That is, any object whose Mahalanobis, Fisher or other statistical distance exceeds a threshold value from the other groups would be categorized as "alien". The representative samples of graded wheats have had very small amounts of this material.

More regularly-shaped objects that have appeared in available samples have been investigated.

3.4 CEREAL, WEED SEED, AND OILSEED DISCRIMINATION-INITIAL STUDY

In an initial study, the feasibility of identifying common contaminants of wheat samples using size and shape features was established. Discrimination among the most frequently occurring of the weed seed, oilseed and cereal contaminants, namely, wild Oats, Canola, Barley, Durum and Rye from Wheat was attempted using four metric properties: perimeter length, contour area, number of contour pixels and thinness ratio. Of the cereal contaminants, Barley appears most often, while the other crops may be expected to appear in order of their relative acreage of production (Table 3.2).

Between 96 and 100 LR kernel images of each species were acquired and processed. These were used to develop a linear classifier whose performance was evaluated by resubstitu-

Table 3.2

Acreage of Crop Grown[1]

Crop	Acreage[2]	(Percent)
Bread Wheats	27.550	(49.19)
Barley	11.050	(19.73)
Canola	7.050	(12.59)
Durum	4.168	(7.44)
Oats	3.650	(6.52)
Flax	1.739	(3.11)
Rye	0.796	(1.42)

[1]Source: Prairie Grain Variety Survey (1984)
Prairie Provinces,1984
[2]Acres x 10^6

tion. The results of linear discriminant analysis applied to the total training set of the 584 contours generated are summarized in Table 3.3.

Greater than 95% correct classification of training samples was achieved for Canola (100% correctly classified), wild Oats (97.0%) and Hard Red Spring Wheat (96.9%). For Barley, the most frequent cereal contaminant, 89.6% of the samples were correctly classified while Durum (60.4%) and Rye (69.8%) were poorly classified. The overall error rate was 14.2% for all classes and 20.8% for the cereals only.

These results indicated that the small oilseeds and large weed seeds could easily be differentiated from wheat on the basis of few characteristics. Flax seeds, being even smaller than rapeseed and similarly round in shape are also clearly distinguishable from the cereals. The data recently reported by Travis and Draper shows that a broad range of weed seeds can be distinguished using features similar to those of this study.

The results of the present study also suggest that resolution among the cereals which are "similar" in size and shape to wheat would require more comprehensive shape description. Similarity of shape was considered to mean being roughly elliptical or bilaterally symmetric, having fewer than three or four points of maximum or undefined curva-

Table 3.3
Discrimination of Cereal Grains
Initial Study

To / From Grain Grain	HRS wheat	Durum wheat	Rye	Wild Oats	Barley	Canola
HRS wheat (n=96)	96.9%	3.1%	-	-	-	-
Durum wheat (n=96)	6.3%	60.4%	30.2%	-	3.1%	-
Rye (n=96)	7.3%	22.9%	69.8%	-	-	-
Wild Oats (n=100)	-	-	3.0%	97.0%	-	-
Barley (n=96)	-	7.3%	3.1%	-	89.6%	-
Canola (n=100)	-	-	-	-	-	100.0%

ture, and having a single-valued Hough transform. The materials that pass through a Carter Dockage tester and appear in samples to be graded are necessarily approximately wheat kernel-sized.

3.5 DISCRIMINATION AMONG CEREAL GRAINS

The initial study was followed up by an expanded one which included a greater variety and number of cereals. All cereal and wheat cultivars listed in Table 3.1 were selected for study while Canola and wild Oats, having been shown to be easily distinguishable, were eliminated. Of the cereals, all the most frequently grown cultivars were included. Table 3.4, compiled from the Prairie Grain Variety Survey (1984), shows these ranked in order of percentage of acreage grown.

Since Neepawa is the predominant HRS cultivar grown, samples were obtained from two geographically separate sources; the classification sets, therefore, totalled 23 in number. The training sets consisted of between 48 and 50 grain or kernel images giving, in total, 1108 prototypes. Separately acquired evaluation sets contained identical numbers of each cultivar.

While several different recognition pattern problems were of interest, all cultivars were simultaneously included in the model to provide maximum opportunity for confusion.

Table 3.4

Most Frequently Grown Cereal Varieties

Cereal	Cultivar	(Percent)	Rank
Bread Wheats	Neepawa	(61.8%)	1
	Columbus	(8.1%)	2
	Benito	(6.6%)	3
	Park	(4.0%)	4
	Sinton	(3.9%)	5
	Glenlea	(2.7%)	6
Durum	Wakooma	(50.1%)	1
	Wascana	(33.0%)	2
	Coulter	(8.6%)	3
	Arcola	(<1.0%)	
Oats	Harmon	(28.1%)	1
	Cascade	(16.0%)	2
Barley	Bonanza	(28.0%)	1
	Klages	(18.9%)	2
Rye	Puma	(34.2%)	1
	Cougar	(30.1%)	2
	Gazelle	(5.3%)	6
	Muskateer	(2.1%)	7

Source: Prairie Grain Variety Survey (1984)
Prairie Provinces,1984

Linear discriminant functions were computed for individual cultivars using combinations of shape features; equal prior probabilities were assumed for Bayes classification. Individual cultivars were considered to be correctly classified as to cereal if either the cultivar was correctly identified or classified as belonging to the same cereal class.

The discriminatory capacity of features from each shape description methodology was investigated. Classification results using normalized shape moments of fifth and lower order are summarized in Table 3.5. Those for the Moment Invariants, the Fourier Descriptors up to the tenth harmonic and the Ellipse-fit features follow in Tables 3.6 to 3.8. Of these methods, only the Ellipse-fit parameters retain size information.

The overall error frequency of grain classification for each method was:

Fourier Descriptors:	12.9%
Shape Moments:	18.1%
Moment Invariants:	23.7%
Ellipse-fit features:	24.5%

For each method, the classification accuracies for common Wheat approached 90% and the admixture cereals, collectively, were infrequently (<7%) classified as the aestivum species. In the last respect, the Fourier Descriptors (1.0%), Ellipse-fit features (1.3%) and Shape Moments (2.3%) were significantly better than the Moment Invariants

Table 3.5
Discrimination of Cereal Grains
Moments only (<6th Order)

To From Cereal Cereal	Common wheat	Durum wheat	Rye	Oats	Barley
Common wheat (n=528)	89.0%	9.5%	-	-	1.5%
Durum wheat (n= 192)	9.9%	83.3%	2.6%	3.7%	<1%
Rye (n=144)	3.5%	11.1%	80.6%	2.8%	2.1%
Oats (n=100)	-	21.0%	30.0%	45.0%	4.0%
Barley (n=144)	2.8%	6.9%	6.3%	3.5%	80.6%

Table 3.6
Discrimination of Cereal Grains
Moment Invariants

To From Cereal Cereal	Common wheat	Durum wheat	Rye	Oats	Barley
Common wheat (n=528)	90.0%	7.8%	<1%	-	1.5%
Durum wheat (n= 192)	38.5%	47.4%	5.7%	<1%	7.8%
Rye (n=144)	11.8%	17.4%	66.0%	-	4.9%
Oats (n=100)	2.0%	21.0%	3.0%	47.0%	27.0%
Barley (n=144)	4.9%	5.6%	1.4%	4.2%	84.0%

Table 3.7
Discrimination of Cereal Grains
Fourier Descriptors

To / From Cereal	Common wheat	Durum wheat	Rye	Oats	Barley
Common wheat (n=528)	91.1%	8.9%	-	-	-
Durum wheat (n= 192)	9.4%	81.8%	6.7%	2.1%	-
Rye (n=144)	1.4%	4.2%	90.3%	<1%	3.5%
Oats (n=100)	-	1.0%	11.0%	84.0%	4.0%
Barley (n=144)	1.4%	1.4%	4.2%	4.9%	88.2%

Table 3.8
Discrimination of Cereal Grains
Ellipse-fit Features

To From Cereal Cereal	Common wheat	Durum wheat	Rye	Oats	Barley
Common wheat (n=528)	87.7%	6.4%	<1%	-	5.5%
Durum wheat (n= 192)	13.5%	50.0%	8.3%	6.8%	21.4%
Rye (n=144)	2.1%	16.7%	77.8%	2.1%	1.4%
Oats (n=100)	-	14.0%	18.0%	50.0%	18.0%
Barley (n=144)	1.4%	9.0%	<1%	8.3%	80.6%

(6.7%). Classification accuracies for the non-Wheat cereals were low ranging from 45 to 91%, the highest accuracies being achieved with Fourier Descriptors. Using as criteria the minimum classification error frequency, correct wheat classification and minimum false labelling of admixture cereals as common wheat, Fourier descriptors and Shape moments gave the best over-all performance.

As no single method provided satisfactory wheat discrimination, all previous data was combined and supplemented with the features: length, width, perimeter length, area, total contour energy, average energy, and aspect and thinness ratios. Classification performance was significantly improved by these additions; the grain classification error was reduced to 2.5%. Results of discriminant analysis using all features are shown in Table 3.9. Greater than 98% of all non-Durum Wheat, Oats and Barley samples were correctly categorized while Durum (97.4%) and Rye (88.2%) were classified less accurately. None of the 576 non-wheat constituents were misclassified as wheat. All of the fewer than 1% falsely-labelled "common" wheat kernels were classed as Durum wheat.

When the least discriminatory feature classes, i.e. the Moment Invariants and Ellipse features and the noise-affected fourth and fifth moments were excluded, the results of Table 3.10 were obtained; average grain classification error was further reduced to 1.8%. This slight improvement

Table 3.9
Discrimination of Cereal Grains
All Features (58)

To From Cereal Cereal	Common wheat	Durum wheat	Rye	Oats	Barley
Common wheat (n=528)	99.6%	<1%	-	-	-
Durum wheat (n= 192)	-	97.4%	2.6%	-	-
Rye (n=144)	-	11.8%	88.2%	-	-
Oats (n=100)	-	-	1.0%	98.0%	1.0%
Barley (n=144)	-	1.4%	-	-	98.6%

indicates that the inclusion of non- discriminating features degrades the classifier performance. The remaining "core" set consisting of Fourier descriptors, low order moments and the additional features listed above has the discriminating capacity of the entire set.

To systematically reduce the dimensionality of the feature space further while retaining high wheat classification accuracy, stepwise discriminant analysis was first applied to generate a ranking of features. Listed in Table 3.11 in their order of addition to the discriminant model are all features whose significance of change to Wilks' lambda exceeds 15.0%. The "shape-space" could be reduced to as few as eight dimensions before wheat tended to be misclassified as barley. Classification results using this reduced feature set are summarized in Table 3.12.

While Rye (81.3%) and Durum wheats (87.5%) were less frequently correctly identified, correct classification of non-Durum Wheats, Oats and Barley again exceeded 99%. Confusion among all grains except non-Durum wheats generally increased. The Canadian wheat grading system is tolerant of this confusion as admixture grains are lumped as one evaluation category.

The discrimination capacity of the single best feature, rectangular aspect ratio, is apparent in Table 3.13. Greater than 95% of wheat and oats kernels could be correctly

Table 3.10
Discrimination of Cereal Grains
(Reduced Feature Set)

To From Cereal Cereal	Common wheat	Durum wheat	Rye	Oats	Barley
Common wheat (n=528)	99.8%	<1%	-	-	-
Durum wheat (n= 192)	-	96.4%	3.1%	-	<1%
Rye (n=144)	-	6.3%	93.1%	-	<1%
Oats (n=100)	-	-	-	99.0%	1.0%
Barley (n=144)	-	<1%	-	-	99.3%

Table 3.11
Ranking of Features by
Stepwise Discriminant Analysis

Variable entered	Number in	F-statistic	Prob >F	Wilks' Lambda
Aspect Ratio	1	950.816	0.0001	0.04931159
Width	2	168.422	0.0001	0.01116110
Four. Des. (-1)	3	195.229	0.0001	0.00224756
Perimeter Length	4	88.517	0.0001	0.00080276
Length	5	33.864	0.0001	0.00047524
Sh. Mom. (0,2)	6	38.310	0.0001	0.00026693
Aspect Ratio (Eig.)	7	23.512	0.0001	0.00018043
Sh. Mom. (2,1)	8	28.077	0.0001	0.00011470
Four. Des. (4)	9	18.607	0.0001	0.00008311
Four. Des. (-4)	10	21.055	0.0001	0.00005810
Thinness Ratio	11	21.131	0.0001	0.00004056
Contour Pixel No.	12	22.596	0.0001	0.00002773
Sh. Mom. (1,2)	13	20.508	0.0001	0.00001952
Area	14	15.374	0.0001	0.00001484
Mom. Inv. 2	15	14.786	0.0001	0.00001138
Mom. Inv. 1	16	20.132	0.0001	0.00000805
Four. Des. (-3)	17	8.947	0.0001	0.00000680
Sh. Mom. (2,0)	18	7.629	0.0001	0.00000587
Sh. Mom. (4,0)	19	7.172	0.0001	0.00000512
Mom. Inv. 3	20	6.969	0.0001	0.00000447
Mom. Inv. 5	21	9.926	0.0001	0.00000371
Four. Des. (-2)	22	5.800	0.0001	0.00000332
Sh. Mom. (5,0)	23	5.237	0.0001	0.00000299
Sh. Mom. (3,0)	24	10.607	0.0001	0.00000245
Mom. Inv. 4	25	6.088	0.0001	0.00000218
Four. Des. (7)	26	5.046	0.0001	0.00000197
Four. Des. (-8)	27	4.634	0.0001	0.00000180

Table 3.11 (cont.)
Ranking of Features by
Stepwise Discriminant Analysis

Variable entered	Number in	F-statistic	Prob >F	Wilks' Lambda
Sh. Mom. (0,3)	28	4.488	0.0001	0.00000164
Four. Des. (-5)	29	4.235	0.0001	0.00000151
Four. Des. (2)	30	4.208	0.0001	0.00000139
Four. Des. (-9)	31	4.076	0.0001	0.00000128
Sh. Mom. (0,5)	32	3.438	0.0001	0.00000119
Semi-Major Length	33	3.232	0.0001	0.00000112
Four. Des. (3)	34	3.150	0.0001	0.00000105
Four. Des. (5)	35	3.272	0.0001	0.00000098
Mom. Inv. 6	36	2.772	0.0001	0.00000093
Energy/Length	37	2.569	0.0001	0.00000088
Four. Des. (-10)	38	2.409	0.0003	0.00000084
Four. Des. (-7)	39	2.133	0.0018	0.00000080
Four. Des. (10)	40	2.031	0.0034	0.00000077
Four. Des. (8)	41	1.828	0.0113	0.00000074
Four. Des. (9)	42	1.793	0.0138	0.00000071
Energy (Total)	43	1.756	0.0170	0.00000069
Eliipse Area Dev.	44	1.625	0.0345	0.00000067
Four. Des. (-6)	45	1.650	0.0302	0.00000064
Four. Des. (6)	46	1.626	0.0342	0.00000062
Sh. Mom. (2,2)	47	1.518	0.0593	0.00000060
Semi-minor Axis L.	48	1.821	0.0118	0.00000058
Mom. Inv. 7	49	1.716	0.0212	0.00000056
Sh. Mom. (1,3)	50	1.538	0.0537	0.00000054
Fitted Ellipse Area	51	1.565	0.0469	0.00000052
Sh. Mom. (2,3)	52	1.450	0.0823	0.00000051
Sh. Mom. (3,1)	53	1.401	0.1034	0.00000049

Table 3.12
Discrimination of Cereal Grains
(8 Most Discriminatory Features)

To From Cereal Cereal	Common wheat	Durum wheat	Rye	Oats	Barley
Common wheat (n=528)	99.2%	-	-	-	<1.0%
Durum wheat (n= 192)	-	81.3%	10.9%	-	7.8%
Rye (n=144)	-	11.8%	87.5%	-	<1%
Oats (n=100)	-	-	-	100.0%	-
Barley (n=144)	-	<1.0%	-	-	99.3%

classified using this single feature. These results confirm the observations of Travis and Draper.

The cereal grain size features vary more than the "shape" characteristics which are used for identification. Large size differences exist even between kernels on an individual stalk. Moreover, the grain size statistics are more likely to be affected by the cleaning process and dockage tests. Therefore, a classifier using "pure" shape features (invariant to kernel size) was developed. High classification accuracies were again achieved (Table 3.14). Wheat was correctly classified for 99.8% of the 528 kernels tested and barley was rarely (1.4%) misclassified as wheat.

Finally, the shape data generated from the "core" feature set was reorganized by cereal, discriminant analysis was performed and the Mahalanobis distances between cereals were obtained. While some confusion between Rye and Durum (Table 3.15) is evident, the remaining cereals are at least piecewise linearly separable in the 35-feature hyperspace. The interclass distances, summarized in Table 3.16, are normalized by the maximum cereal separation from Common Wheat which is taken to be 100 units. By this index, Barley (100) is by far the most dissimilar to wheat, followed in order by Oats (27.4), Rye (13.9) and Durum (5.1).

Table 3.13
Discrimination of Cereal Grains
Aspect Ratio

To From Cereal Cereal	Common wheat	Durum wheat	Rye	Oats	Barley
Common wheat (n=528)	95.8%	<1%	-	-	3.4%
Durum wheat (n= 192)	<1%	68.7%	9.4%	-	21.4%
Rye (n=144)	-	26.4%	27.8%	-	45.8%
Oats (n=100)	-	-	-	96.0%	4.0%
Barley (n=144)	2.1%	52.8%	9.0%	1.4%	34.7%

Table 3.14
Discrimination of Cereal Grains
(Shape Features Only Used)

To From Cereal Cereal	Common wheat	Durum wheat	Rye	Oats	Barley
Common wheat (n=528)	99.8%	<1.0%	-	-	-
Durum wheat (n= 192)	-	94.8%	5.2%	-	-
Rye (n=144)	-	6.9%	93.1%	-	-
Oats (n=100)	-	-	-	100.0%	-
Barley (n=144)	1.4%	1.4%	1.4%	-	95.8%

Table 3.15
Discrimination of Cereal Grains
(Data Grouped By Cereal)

To From Cereal Cereal	Common wheat	Durum wheat	Rye	Oats	Barley
Common wheat (n=528)	98.3%	1.7%	-	-	-
Durum wheat (n= 192)	-	97.4%	2.1%	<1%	-
Rye (n=144)	-	9.0%	91.0%	-	-
Oats (n=100)	-	-	-	99.9%	1.0%
Barley (n=144)	-	2.1%	-	-	97.9%

Table 3.16
Mahalanobis Distances
-normalized to Wheat-Barley (100 units)

To From Cereal Cereal	Common wheat	Durum wheat	Rye	Oats	Barley
Common wheat	0.00	5.08	13.92	27.37	100.00
Durum wheat	-	0.00	5.99	19.70	73.64
Rye	-	-	0.00	22.02	63.66
Oats	-	-	-	0.00	107.01
Barley	-	-	-	-	0.00

3.6 DISCRIMINATION AMONG WHEAT CLASSES AND VARIETIES

Further analyses of the wheat classification results were made to investigate the capacity of shape to distinguish between wheat cultivars and classes. The wheat classes considered were Hard Red Spring (HRS), Hard Red Winter (HRW), Soft White Spring (SWS), Utility, Prairie Spring (PS) and Durum Wheats. The five most commonly grown varieties (Table 3.4, page 63), collectively comprising more than 80% of the acreage grown, of the predominant Hard Red Spring class were included. Cultivars were considered to be correctly labelled as to class if either correctly identified or classified as another cultivar of the same class. The results, using all available shape data, are shown for each cultivar in Table 3.17 and grouped by class in Table 3.18.

These results likely represent the maximum classification accuracies achievable with a linear classifier based solely on shape. Correct classification by class was high for HRS wheat (98.9%) and Durum wheats (97.4%). On average, wheat of the remaining classes was poorly classified (53.3 %). While confusion among these classes was high, none were categorized as HRS wheat. The non-HRS wheats are collectively counted in the "wheat of other classes" category for wheat grading purposes.

Reduction of the feature set is possible without loss of HRS discrimination. When Moment Invariants, Ellipse-fit

features and high order moments were again eliminated, the confusion pattern was unchanged. Durum and HRS classifications were slightly diminished (Tables 3.19 and 3.20).

For wheat grading, identification of unlicensed HRS or utility varieties is required. In general, individual wheat varieties could not be accurately identified using shape information (Table 3.21). The low accuracies for individual HRS varieties are attributable to their being bred to be visually indistinguishable. The licensed utility wheat Glenlea, which has a distinctive elongated shape was correctly identified for 75% of samples. Notably, other hard red varieties Norstar (HRW) and Hy320 (PS semi-dwarf) while not identified were at least distinguishable from the HRS class as a whole.

3.7 DISCRIMINATION AMONG NON-WHEAT VARIETIES

While wheat grading is of primary importance, the cereal discrimination results apply equally to grading of other grains. The grading factors and objects that are identified in Barley, Oats and Rye largely parallel those of wheat (OGGG, 1985). Of these cereals, the Barley varieties and Harmon Oats could be discerned with relatively high frequency (>80%, Table 3.21). The Rye varieties and Fidler Oats were correctly labelled less often having classification accuracies ranging from 42% to 62%. These are nevertheless high in relation to the 4.3% to 4.5% prior probabilities of selection.

Table 3.17
Classification of Wheat Cultivars into Grain Classes
All Features Used

From Cultivar	To Class	HRS	HRW	SWS	Utility	PS	Durum	Other Cereals
HRS	Neepawa_a	100.0%	-	-	-	-	-	-
	Neepawa_b	93.8%	-	4.2%	2.1%	-	-	-
	Katepwa	100.0%	-	-	-	-	-	-
	Columbus	100.0%	-	-	-	-	-	-
	Benito	100.0%	-	-	-	-	-	-
	Park	100.0%	-	-	-	-	-	-
HRW	Norstar	-	56.3%	25.0%	2.1%	16.7%	-	-
SWS	Fielder	-	27.1%	45.8%	8.3%	18.8%	-	-
	Owens	-	2.1%	64.6%	14.6%	18.8%	-	-
Util.	Glenlea	-	-	8.3%	75.0%	14.6%	2.1%	-
PS	Hy320	-	-	29.2%	43.8%	25.0%	2.1%	-
Durum	Coulter	-	-	-	-	-	97.9%	2.1%
	Wakooma	-	-	-	-	-	95.8%	4.2%
	Wascana	-	-	-	-	-	95.8%	4.2%
	Arcola	-	-	-	-	-	100.0%	-

Table 3.18
Discrimination of Wheat Classes
(All Features Used)

From Class \ To Class	Hard Red Spring	Hard Red Winter	Soft White Spring	Utility	Prairie Spring	Durum	Other Cereals
Hard Red Spring (n=288)	98.9%	-	<1%	<1%	-	-	-
Hard Red Winter (n= 48)	-	56.3%	25.0%	2.1%	16.7%	-	-
Soft White Spring (n= 96)	-	14.6%	55.2%	11.5%	18.8%	-	-
Utility Wheat (n= 48)	-	-	8.3%	75.0%	14.6%	2.1%	-
Prairie Spring (n= 48)	-	-	29.2%	43.8%	25.0%	2.1%	-
Durum Wheat (n= 192)	-	-	-	-	-	97.4%	2.6%

Table 3.19
Classification of Wheat Cultivars into Grain Classes
Reduced Feature Set

From Cultivar	To Class	HRS	HRW	SWS	Utility	PS	Durum	Other Cereals
HRS	Neepawa_a	100.0%	–	–	–	–	–	–
	Neepawa_b	91.7%	–	6.3%	2.1%	–	–	–
	Katepwa	100.0%	–	–	–	–	–	–
	Columbus	100.0%	–	–	–	–	–	–
	Benito	97.9%	–	–	2.1%	–	–	–
	Park	97.9%	–	2.1%	–	–	–	–
HRW	Norstar	–	31.3%	52.1%	2.1%	14.6%	–	–
SWS	Fielder	–	10.4%	66.7%	10.4%	12.5%	–	–
	Owens	–	2.1%	79.2%	14.6%	4.2%	–	–
Util.	Glenlea	–	–	12.5%	75.0%	10.4%	2.1%	–
PS	Hy320	–	–	37.5%	39.6%	22.9%	–	–
Durum	Coulter	–	–	–	–	–	97.9%	2.1%
	Wakooma	–	–	–	–	–	93.7%	6.3%
	Wascana	–	–	–	–	–	95.8%	4.2%
	Arcola	–	–	–	–	–	97.9%	2.1%

Table 3.20
Discrimination of Wheat Classes
-Reduced Feature Set

From Class / To Class	Hard Red Spring	Hard Red Winter	Soft White Spring	Utility	Prairie Spring	Durum	Other Cereals
Hard Red Spring (n=288)	97.9%	-	1.4%	<1%	-	-	-
Hard Red Winter (n= 48)	-	31.3%	52.1%	2.1%	14.6%	-	-
Soft White Spring (n= 96)	-	6.3%	72.9%	12.5%	8.3%	-	-
Utility Wheat (n= 48)	-	-	12.5%	75.0%	10.4%	2.1%	-
Prairie Spring (n= 48)	-	-	37.5%	39.6%	22.9%	-	-
Durum Wheat (n= 192)	-	-	-	-	-	96.3%	3.7%

Table 3.21
Discrimination of Cereal Grains
Cultivar Identification

Wheat class	Cultivar	Correctly identified	Grain	Cultivar	Correctly identified
HRS	Neepawa-a	98%	Durum	Wakooma	31%
	Neepawa-b	69%	wheat	Wascana	50%
	Katepwa	67%		Arcola	88%
	Columbus	19%		Coulter	60%
	Benito	48%			
	Park	75%	Barley	Bonanza	88%
				Klages	94%
HRW	Norstar	31%		Johnston	83%
PS	HY320	23%	Oats	Fidler	62%
				Harmon	86%
Utility	Glenlea	75%			
			Rye	Gazelle	42%
SWS	Fielder	50%		Muskateer	58%
	Owens	73%		Puma	52%

1. Based on a training and evaluation set of 48 kernels respectively.
2. Grain samples of Neepawa obtained from two sources.
3. Abbreviations: Hard Red Spring (HRS), Hard Red Winter (HRW), Prairie Spring (PS), Soft White Spring (SWS)

3.8 DISCRIMINATION AMONG UNSOUND KERNELS

A further inquiry was made to determine whether certain characteristically damaged or degraded kernels could be distinguished from sound kernels by size and shape differences. Included for study were shrunken, broken and sprouted kernels of HRS wheat each representing a separate grading category. These, apart from frost-damaged and bleached kernels, are the most frequently occurring unsound species.

In total, 96 LR images of each were acquired and processed. All shape descriptors were computed including symmetry attributes. A linear classifier was developed and evaluated by the hold-out method with the results summarized in Table 3.22.

The broken (95.8%) and sprouted groups (99.0%) were successfully identified. Broken kernels were most often misclassified as shrunken. The broken kernels included in this study were any with apparent fracture; many exceeded the "three-quarters of a whole kernel" defining threshold. Therefore kernels with very minor breakage and minimal sprouting were resolved.

However, considerable confusion between shrunken and sound kernels is evident.

Table 3.22
Kernel Soundness

To / From	Broken	Shrunken	Sound	Sprouted
Broken (n= 96)	95.8%	3.1%	0	1.0%
Shrunken (n= 96)	0	87.5%	12.5%	0
Sound (n= 96)	0	9.4%	90.6%	0
Sprouted (n= 96)	1.0%	0	0	99.0%

Chapter IV

CONCLUSIONS AND RECOMMENDATIONS

The objective of the work described in this thesis has been to investigate the capacity of machine-vision perceivable size and shape characteristics to differentiate elements that must be quantified for wheat grading purposes. This research has proceeded in parallel with that on texture and light transmission characteristics performed by others (Wright, 1985, Sapirstein et al, 1985). Specific problems that have been posed for experimental resolution are:

1. distinguishing other cereal grains, oilseeds and weed seeds from wheat
2. distinguishing other wheat classes from Red Spring Wheat
3. distinguishing certain categories of damaged RS wheat from mature sound wheat kernels
4. the capacity of size and shape to distinguish individual cultivars not only of wheat but also of other cereals.

For the first time, machine perceivable kernel size and shape characteristics have been used to discriminate between commonly grown Canadian oilseeds, wheat and cereal varieties. Further, their use for distinguishing between un-

sound and sound wheat kernels has not been previously described. Previous studies that have attempted to discriminate among various cereals and/or weed seeds have primarily employed either size or shape characteristics but not both. Also unlike the approach taken herein, with one exception (Segerlind and Weinberg, 1972), no effort has been made to use all information present in the seed shape. Whereas all past studies of seed shape have required extensive manual involvement in orienting kernels, extracting contours or taking measurements, activities which inhibit their use for automatic grading, these tasks have either been avoided or accomplished automatically by the described methods.

Discrimination of contaminating cereals from wheat was achieved using a rapidly computable set of shape and size features. All major methodologies of contour shape description were applied to this problem. The best results were achieved using a set of features which included Fourier descriptors, low order shape moments, rectangular aspect ratio and length, width and area measures. Correct cereal classification using this set of features were :

Non-durum wheats:	99.8%
Durum wheats:	96.4%
Oats:	99.0%
Rye:	93.1%
Barley:	99.3% .

When size features were eliminated from this set, i.e. only shape dependent features were used, cereal classification performance deteriorated only slightly; the overall error rate was 2.4 % as compared with 1.8 %. If only the eight most discriminatory features were used, confusion among all cereals but the non-Durum wheats increased. For these wheats of primary interest for wheat grading, classification exceeded 99%.

The most common oilseed (Canola) and weed seed (Wild Oats) were easily distinguished from all other cereal classes on the basis of four features. While shrunken kernels were occasionally confused with sound kernels, broken and sprouted kernels were not. The high classification accuracies achieved for certain wheat and cereal cultivars despite low prior probabilities indicate that certain cultivars such as Neepawa and Glenlea or Neepawa and semi-dwarf varieties might be reliably separated on a pairwise basis. To verify this, further study will be required on a wider range of samples of different provenance.

The research may be extended in several other ways which include improvements and modifications to the image acquisition system, expansion of features extracted from the system and consideration of other pattern recognition methodologies. The existing experimental system, with certain improvements, could be developed into a real-time wheat analysis system, the ultimate goal of the research effort. Shape

analysis routines may be implemented in assembly language and discriminant functions rapidly computed and compared on-board avoiding time consuming image transfer. In future, the intrinsic parallelism of the procedures may be exploited to simultaneously analyze many objects within the image. At present, the single time-limiting manual procedure is the placement of samples on the optical platform. This procedure might be eliminated by suitable adaptation of the sample acquisition system described by Brogan and Edison (1974).

Colour imagery is the most desirable system modification in that a broader range of recognition problems could be proposed including the finding of grass-green, pink, stained, dark immature, vitreous, insect and fungus-affected kernels. Discrimination among Amber durum, Red and White wheats would likely be enhanced using tristimulus values integrated over individual kernels. Therefore, in synergy, shape and colour characteristics may suffice to identify objects in a large fraction of the categories quantified for wheat grading purposes .

In the absence of colour, only monochrome texture features may presently be extracted from the digital images. In general, such features are very illumination sensitive being affected by specular reflection and mutual and self-shadowing of image constituents. Under carefully controlled illumination and sample orientation conditions, Wright (

1985), using autoregression modelling, failed to discriminate between mature vitreous and "wrinkled" unsound kernels. This result suggests that texture analysis would contribute only marginally to the major discrimination problems of wheat grading for which visual texture differences are much less evident. However, two additional approaches might be considered for specific problems. The grey level run length features described by Galloway (1975) might resolve the previously-mentioned shrivelled or "wrinkled" wheat. The moment method described in this thesis can be extended to use the grey level information within the contour boundary (Tang, 1981). Such grey level moments, which give the distributional shape of ranges of pixel intensity, might be applied to finding "blackpoint"-affected kernels or other conditions that affect local appearance of the kernel.

Entirely apart from the addition of new features, other pattern recognition methodologies may be considered. The present study was conducted in the supervised learning mode since training samples were readily available. An alternative recursive self-learning approach, particularly that using Kalman filtering (Brogan and Edison, 1974) might be applied to "real" wheat samples. A more important requirement is the introduction of a loss function (Tou and Gonzalez, 1974) to reflect the unequal costs of misclassification. The misidentification of an ergot-affected kernel, for example, may be more significant than that of a contaminating barley kernel.

In this thesis, a single stage classifier was developed to simultaneously discriminate among a large number of wheat cultivars. This problem may be restructured using multistage classification which has recently received much attention in the pattern recognition literature. At each stage of classification, corresponding to the level of an hierarchical tree, a pattern is compared with a set of classes. Each such comparison, represented by a tree node, determines whether testing paths emanating from that particular node will be followed. Paths which result in the comparison of a pattern with unlikely subclasses are ignored resulting in the rapid exclusion of many alternatives. However, all comparison branches are followed for which the likelihood exceeds a prescribed level; i.e unlike a decision tree, more than one parallel path may be followed. For each node, a much smaller number of features optimized for the partial discrimination problem are used than would be for an overall single stage classifier.

In illustration, the overall wheat grading procedure might be performed in stages. An object in a wheat sample image could first be classified as either "wheat" or "non-wheat". If chosen as the latter, a determination of "foreign cereal" against "alien matter" would be made and more specific identification would follow by comparisons made in one of the two alternative test branches. The "alien" path might include such categories as weed seeds, oilseeds, in-

sect ova, larvae and adults, excreta, machine bolts and an unlimited range of other rare objects that could be added to the substage class set as experience is gained.

Similarly, if the object is wheat, then it might undergo a sequence of comparisons to determine the likelihood of its

1. belonging to either aestivum or durum species
2. if the former, belonging to the Red Spring or White class
3. if Red Wheat, whether it is damaged or adversely affected in any way.

Of course, this is just one of many possible comparison structures and is not optimal in any way. Kurcynski (1983) has developed a strategy for the design an hierarchical classifier to minimize the overall probability of error given complete problem probabilistic information. Implicitly, a single stage classifier developed from training data may be recast as an optimal multistage classifier.

The development of an appropriate multistage classifier for wheat grading would likely be the most fruitful direction of pattern recognition research. Such a classifier, unlike a single stage one, could accommodate the broad range of objects that must be correctly identified in a wheat sample for accurate grading. The conformity of hierarchical classifiers with human decision procedures makes them especially attractive in the context of the development of an overall "expert system" for wheat grading.

LITERATURE CITED

Attneuve, T., Some informational aspects of visual perception, Psychol. Rev., 61, 1954, 183-193

Bennett, J.R. and MacDonald, J.S., On the measurement of curvature in a quantized environment, IEEE Transactions on Computers, C-24, #8, 1975, 803-820

Brogan, W.L. and Edison, A.R., Automatic classification of grains via pattern recognition techniques, Pattern Recognition, 16, 1974, 97-103

Bushuk, W., "Wheat around the world", p357-477, In: Grains and Oilseeds: Handling, Marketing and Processing, Canadian International Grains Institute, Winnipeg, 1977

Chen, C.Y., Skarsaune, S.K. and Watson, C.A., Relation of kernel colour to wheat class and grade, Cereal Science Today, 17, 1972, 340-343

Chuan-Juan, C. and Qing-Yun, S., Shape features for cancer cell recognition, In: Proceedings of the 5th International Conference on Pattern Recognition, IEEE Computer Society Press, 1981 , 579-581

Draper, S.R. and Travis, A.J., Preliminary observations with a computer-based system for analysis of the shape of seeds and vegetative structures, Journal of the National Institute of Agricultural Botany, 16, 1984, 387-395

Dudani, S.A., Breeding, K.J. and McGhee, R.B., Aircraft identification by moment invariants, IEEE Transactions on Computers, C-26, 1977, 39-46

Edison, A.R. and Brogan, W.L., Size measurement statistics of kernels of six grains, Paper No. 72-841, The 1972 Winter Meeting, American Society of Agricultural Engineers, Chicago, Illinois, 1972

Freeman, H., On the encoding of arbitrary geometric configurations, IRE Transactions on Electronic Computers, 10, 1961, 260-268

Galloway, M., Texture analysis using gray level run lengths, Computer Graphics and Image Processing, 4, 1975, 172-179

Gonzalez, R.C. and Wintz, P., Digital Image Processing, Addison Wesley , London, 1977

Haralick, R.M., Statistical and structural approaches to texture, Proc. IEEE, 67, 1979

Hawk, A.L., Kaufmann, H.H. and Watson, C.A., Reflectance characteristics of various grains, Cereal Science Today, 15, 1970, 381-384

Hu, M., Visual pattern recognition by moment invariants, IRE Transactions on Information Theory, 1962, 179-187

Inguanzo, J.M., Pattern Recognition Techniques for Automatic Classification of Grains, PHD thesis, University of Nebraska, 1977

Kurcynski, M.W., The optimal strategy of a tree classifier, Pattern Recognition, 16, 1983, 81-87

Official Grain Grading Guide, (OGGG), Office of the Chief Grain Inspector, Inspection Division, Canadian Grain Commission, Winnipeg Manitoba, 1985

Owens, C.H. and Ainslie, M.M., Varietal Identification of Barley, Wheat and Small Oilseeds by Kernel Characters, Canadian Grain Commission, Winnipeg, Manitoba, 1971

Pavel, M., "Shape theory" and pattern recognition, Pattern Recognition, 16, 1985, 349

Pavladis, T., A review of algorithms for shape analysis, Computer Graphics and Image Processing, 7, 1978, 243-258

Prairie Grain Variety Survey (PGVS), Canadian Co-operative Wheat Producers, Ltd., Regina, 1984

Preston, K. and Onoe, M., Eds., Digital Processing of Biomedical Images, Plenum Press, New York, 1976

Reeves, A.M. and Rostampour, A., Shape analysis of segmented objects using moments, In: Proceedings on Pattern Recognition and Image Processing, IEEE Computer Science Press, New York, 1981, 171-174

SAS, SAS User's Guide: Statistics, SAS Institute Inc., Cary, North Carolina, 1982

Sapirstein, H.D. and Bushuk, W., Computer-aided analysis of electrophoregrams. II. Wheat cultivar identification and class comparisons, Cereal Chemistry, 62, 1985, 377-392

Sapirstein, H.D., Wright, E., Neuman, M., Schwedyk, E. and Bushuk, W., Wheat Grading by Computer Image Analysis, Address to: The 10th Joint Conference of Operative Millers (District No. 13) and American Association of Cereal Chemists (Canadian Prairie Section), Winnipeg, Manitoba, Sept. 11-13, 1985

Segerlind, L. and Weinberg, B., Grain kernel identification by profile analysis, Paper No. 72-314, The 1972 Annual Meeting, American Society of Agricultural Engineers, 1972

Tang, G.Y., A discrete version of Green's theorem, In: Proceedings on Pattern Recognition and Image Processing, IEEE Computer Science Press, 1980, 144-149

Tatsuoka, M.M., Discriminant Analysis, Institute for Personality and Ability Testing, Champaign, Illinois, 1970

Tou, J.T. and Gonzalez, R.C., Pattern Recognition Principles, Addison-Wesley, London, 1974

Travis, A.J. and Draper, S.R., A computer based system for the recognition of seed shape, (to be published)

University of Manitoba Kernel Frame Grabber Manual, (UMKFG), Department of Electical Engineering, University of Manitoba, 1985

Wilks, S., Mathematical Statistics, Wiley, New York, 1962

Wong, R.Y. and Hall, E.L., Scene matching with invariant moments, Computer Graphics and Image Processing, 8, 1978, 16

Wright, E., Machine Vision Applied To Wheat Grading: Initial Research, M.Sc. Thesis, University of Manitoba, 1985

Young, I.J., Walker, J.E. and Bowie, J.E., An analysis technique for biological shape 1. Information and Control, 25, 1974, 357-370

Zahn, C.T. and Roskies, R.Z., Fourier descriptors for plane closed curves, IEEE Transactions on Computers, C-21, 1972, 269-281

Zayas, I., Pomeranz, Y. and Lai, F.S., Discrimination between Arthur and Arkan wheat by image analysis, Cereal Chemistry, 62, 1985, 478-480